Advanced channeling technologies for X-ray applications

Sultan Dabagov[a,b,c,*], Y.P. Gladkikh[d]

[a] INFN - XLab Frascati, Laboratori Nazionali di Frascati, Italy
[b] RAS - P.N. Lebedev Physical Institute, Moscow, Russia
[c] NR Nuclear University MEPhI, Moscow, Russia
[d] Belgorod State University, Belgorod, Russia

ARTICLE INFO

Keywords:
Channeling
X-ray channeling
Polycapillary optics
Microchannel plates
X-ray elemental analysis
X-ray imaging

ABSTRACT

Recent studies have shown the feasibility of channeling phenomenology applications to describe various mechanisms of interaction of charged and neutral particle beams and radiations as well in solids, plasmas, laser fields - in general, in external electromagnetic fields. As proved, X-rays and thermal neutrons propagation in metamaterials composed by hollow multichannel substance can be much easily analyzed within channeling theory. Its utilization allows predicting some new peculiarities in the radiation distribution behind multichannel subjects that might create novel fine instruments and methods for future applied techniques.

1. Introduction

Crystal-lattice bound motion of charged particles in aligned crystals is known as channeling of charged particles. Additional to deep interests of the researchers to the basic peculiarities of such motion, since its discovery the beams channeling has been studied as an efficient tool to shape the beams of charged particles at large accelerators, storage rings and colliders. Channeling is also a powerful technique to make the beams undulating in very limited transverse space that becomes an interesting tool as a radiation source.

Beams of relativistic charged particles moving in crystals along crystallographic planes or axes under small glancing angles might interact coherently with large number of lattice atoms/ions. The interaction of these particles with a crystal is defined by averaging the "projectile - atom/ion" interaction over the atoms distribution either in a plane or in an axis, respectively. This procedure introduces an averaged interaction potential, so-called "continuous potential", planar or axial one. The motion in such a potential is fast oscillating. It is nonrelativistic in transverse space, which is limited within well defined channels. In the same time, longitudinal motion down long-narrow channels remains relativistic. Presently this phenomenon in solids is known as channeling of beams in crystals (Lindhard, 1965; Gemmell, 1974; Davies, 1974).

For many years of intense studies the basics of crystal channeling for charged beams have been in detail defined and described in many scientific papers and books (Kumakhov and Shirmer, 1979; Baryshevsky, 1982; Ohtsuki, 1983; Bazylev and Zhevago, 1987; Kalashnikov, 1988; Baier et al., 1998), discussed in a number of conferences and workshops (see, for instance in (Saenz and Uberall, 1985; Carrigan and Ellison, 1987; Wiedemann, 2005; Dabagov, 2005, 2007, 2010, 2011, 2013, 2015, 2017; Dabagov and Strikhanov, 2013, 2016)). Nowadays crystal channeling is known as useful technique for beam steering (Tsyganov, 1976; Carrigan, 1975), while related radiation phenomena are promising candidates for coherent radiation sources (Kumakhov and Komarov, 1989; Akhiezer and Shul'ga, 1996; Rullhusen et al., 1998). Moreover, the phenomenology of beams channeling has been applied for description of electromagnetic radiation propagation in various guiding structures (Dabagov, 2003a; Bukreeva et al., 2006; Dabagov and Uberall, 2007, 2008). At present we can claim that channeling conditions could be realized for particles in crystals (Biryukov et al., 1997), capillaries (Kumakhov and Komarov, 1990; MacDonald, 2010), nanotubes (Zhevago and Glebov, 2003; Klimov and Letokhov, 1996; Karabarbounis et al., 2013), plasma channels (Esarey et al., 2002; Kostyukov et al., 2003; Faure et al., 2010; Dik et al., 2013)), and in high-intensity periodic electromagnetic fields (Frolov et al., 2013).

Since the middle of 1980s this phenomenology has been applied to describe the features of both X-rays and neutrons propagation in specially designed optical guides, presently known as capillary/polycapillary optics. These types of the optics are typically characterized by a set of artificial long hollow guides of various geometry, transversely space-limited, forming in such a way a multichannel micro- or nanostructure similar to photonics crystals. Capillary based optical systems are known as one of the most potent units to get highly focused or collimated X-ray beams, especially, from laboratory sources. It opens very wide field of applications for both basic and industry investigations. Nowadays, due to developments in micro- and nanotechnologies,

* Corresponding author at: INFN - XLab Frascati, Laboratori Nazionali di Frascati, Italy.
E-mail address: sultan.dabagov@lnf.infn.it (S. Dabagov).

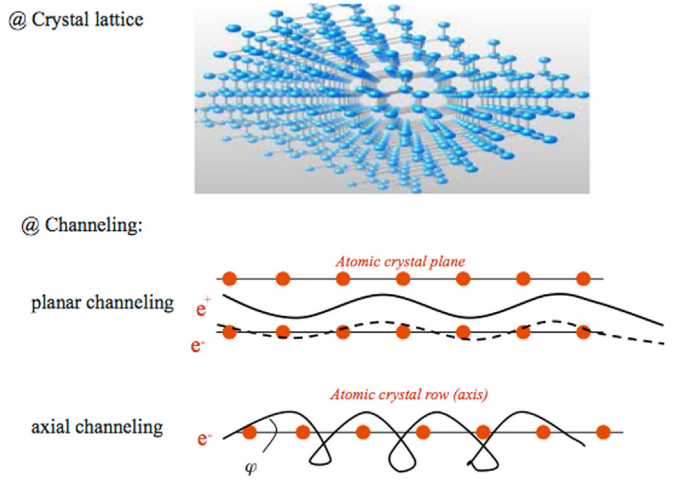

Fig. 1. (a) Scheme for crystal channeling of charged particles. Upper picture demonstrates the crystal lattice composed by the ions (crystal electrons not shown). Two basic types of channeling in crystals, planar and axial, are shown for electrons and positrons.

new samples of microchannel plates (MCP) are under intense studies for their ability to act as efficient X-ray guiding systems.

In this paper, after brief introduction to the physics of charged beams channeling in external electromagnetic fields, we present the phenomenology of X-ray channeling in capillary structures as well as the basics of polycapillary optical elements. Then the high applicability of polycapillary optics is proved by several analyzed applications for X-ray fluorescence and imaging, including the computed tomography (CT). Finally, we discuss the features of X-ray propagation in the channels of MCP samples.

2. Channeling of charged and neutral beams

2.1. Channeling in crystals

In the beginning of 1960s studying the motion of ion beams in crystals via computer simulations has resulted in the prediction of the phenomenon of anomalous beams penetration into the crystals (Robinson and Oen, 1963; Beeler, 1963). Soon after the phenomenon was experimentally proved (Piercy et al., 1963; Lutz and Sizmann, 1963) (Fig. 1), and the phenomenology for a new phenomenon called "channeling" was successfully suggested (Lindhard, 1965) introducing the definitions for "continuous potential" and "critical angle" (known as Lindhard angle) as well as necessary conditions for channeling (Appleton et al., 1967). That work has stimulated great interest of physicists to investigate the effect making soon available both classical and quantum channeling theories. Further studies on beams channeling has been mainly provoked by the prediction of powerful spontaneous γ-radiation by relativistic positrons and electrons channeled in crystals (Kumakhov, 1976). The phenomenon was based on the particle undulation within the potential well determined by the continuous potential (Beloshitsky and Komarov, 1982; Dabagov and Zhevago, 2008).

Due to extremely high field gradient (for instance, the gradient of averaged crystal interaction potential $\delta V/\delta x \sim 10 \div 10^2$ eV/Å $= 0.1 \div 1$ TeV/m^2) the phenomenon becomes rather powerful tool to shape (deflection, steering, splitting) the beams of heavy particles at the modern accelerator facilities. The efficiency of beam collimation is mostly defined by the angular acceptance of aligned crystals,[1] namely by the critical angle, which is inverse proportional to the projectile energy $\varphi_L \propto \gamma^{-1/2}$ (γ is the Lorenz factor). For instance, at planar channeling of $E = 400$ GeV/c protons in Si $\varphi_L \simeq \sqrt{2V_0/E} \sim 10$ μ rad where V_0 and $E = E_0\gamma$ are the potential barrier of planar continuous potential and the projectile energy, respectively (E_0 is the rest particle energy). The use of optimally bent crystals when the radius of curvature is not less than so-called critical radius of crystal bending $R \geq R_c = d_p/(2\varphi_L^2)$ to fulfill the channeling condition $\varphi_i \leq \varphi_L$ for any undulation cycle i (d_p is the transverse channel size), allows the projectiles to be deflected by the angle much over the critical one (typically more than one order difference for relativistic hadrons). Keeping in mind conventional large-scale beam collimation systems, one should underline here that the crystal-based beam deflection over large angles takes place for crystals of several mm thicknesses (Tsyganov, 1976; Carrigan, 1975).

In order to examine the motion of relativistic particles in both straight and bent crystals various computing codes to simulate the processes of relativistic proton/ion beams scattering in the crystal nuclear and electron subsystems have been proposed and developed (see in Babaev et al., 2013; Babaev and Dabagov, 2012, 2011 and Refs. therein). Additionally to the beam deflection by bent crystals another interesting phenomenon, parametric X-ray radiation (PXR), is presently under intense investigation. PXR has been proposed to be used for diagnostics of both beam-crystal orientation and crystal quality. First PXR measurements for SPS CERN (the Super Proton Synchrotron of the European Organization for Nuclear Research) protons in a bent crystal have been performed. They have successfully proved the predictions for PXR making evident the peak structure in both spectral and angular distributions of the radiation (Scandale et al., 2011a; Dabagov et al., 2016; Korotchenko et al., 2017).

At present the use of planar channeling in bent crystals to control a charge particle beam is of great interest as one of the accelerator and storage ring collimation techniques. For the last decade several technologies for crystal collimation have been proposed and developed (single bent crystals and strip crystals in various configurations). During technological testing measurements new phenomena for beam deflection have been observed (channeling, volume capture, volume reflection, etc). While for a long period the experiments have been dealing with the proton beams of 400 GeV/c at SPS CERN revealing the fine features of proton channeling, like beam mirroring, focusing, collimation, the last measurements were performed for LHC (the Large Hadron Collider) proton beams of 6.5 TeV/c proving the feasibility of ultra-relativistic proton channeling in bent crystals (Scandale et al., 2011b, 2013, 2014a, 2014b, 2014c, 2015, 2016).

Recent studies have also shown rather efficient beam deflection for light particles. Indeed, the tests performed at MAMI (the Mainz Microtron) and SLAC (the Stanford Linear Accelerator Center) as well allowed observing very efficient sub-GeV (855 MeV MAMI) and multi-GeV (3.5 and 6.3 GeV) electron beam steering (Mazzolari et al., 2014; Wienands et al., 2015, 2017).

A new phenomenon on effective deflection of relativistic hadron and lepton beams by crystal miscut surface has been also predicted (Babaev et al., 2015a, 2015b). Due to extremely fine structure of the miscut surface the phenomenon might be applied for future accelerators dealing with nanoscale emittances. Successfully the features of crystal miscut have been first used for relativistic pions focusing providing a short focal distance (180 GeV/c focused by 0.5 mm crystal at distance of $\sim$ 16 cm) (Scandale et al., 2018).

2.2. Channeling in optical lattices

The topic of electrons dynamics in crossed laser beams being introduced many years ago still attracts attention of the researchers. Usually in most of the projects the case of standing electromagnetic waves as a result of two counter-propagating laser beams is considered. Kapitza and Dirac were the first who referred to electron dynamics in such an interference field in well known paper (Kapitza and Dirac, 1933) introducing for the first time to electron beam diffraction in standing optical field. Many papers were lately published studying

[1] Obviously, at calculations we have to take into account all scattering processes for a beam in a crystal.

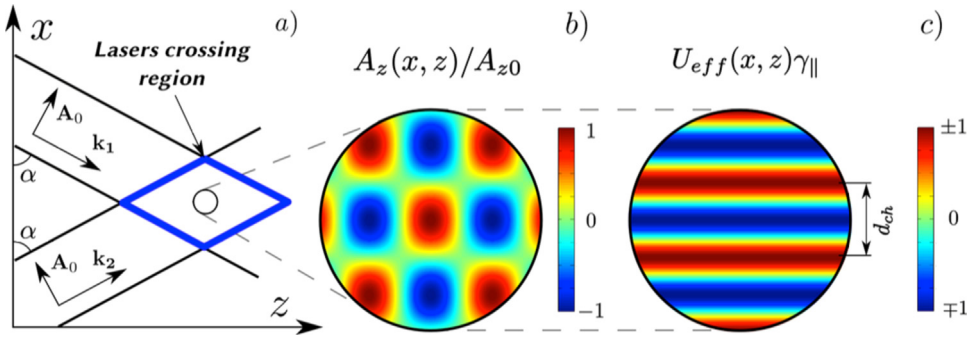

Fig. 2. (a) Scheme of the field for two crossed laser beams. (b) The longitudinal component of summarized vector potential (in arbitrary units) in the central area of lasers crossing region in two plane waves approximation (the case of $\alpha \in (0, \pi/2)$ is shown). The peaks of A_z migrate in the direction of Oz-axis. (c) Normalized effective potential distribution for the same area of (b). The potential absolute value depends on lasers parameters, angle α and electron velocity.

basics of the processes that take place in such systems (Kaplan and Pokrovsky, 2005; Pokrovsky and Kaplan, 2005; Dabagov et al., 2015) as well as proposing a tool for novel free electron lasers based on optical undulator (Fedorov et al., 1988; Balcou, 2010; Andriyash et al., 2011, 2012, 2013), for channeling radiation source (Bertolotti et al., 1986; Andreev and Akhmanov, 1991; Frolov et al., 2013, 2014), for beam monitoring (Shintake, 1992), etc.

The electron motion in optical lattice formed by crossed linearly polarized laser beams, in plane waves approximation, might be described in terms of particle channeling. In the region of two laser beams overlapping at the angle 2α the ponderomotive force characterized by averaged effective potential $U_{eff} = -U_{am}\cos(2kx\cos\alpha)$ with the wave number k, the effective potential amplitude U_{am} affects charged particles. The amplitude $U_{am} = f(A_0, \alpha, \gamma)$ is indeed the function of vector-potential of laser field, cross-angle and particle energy (see in Fig. 2). The ponderomotive potential forms planar (one-dimensional) potential wells. A charged particle might be trapped in such a well resulting in its transverse oscillations once the condition for the angle between particle momentum and channel longitudinal axis $\theta \le \theta_c = p_\perp/p_\| \approx \sqrt{2U_{am}/\gamma mc^2}$ is fulfilled.

We have to underline that there are much in common between particle dynamics in crossed laser and crystal channeling fields. First of all, interference of two crossed laser beams creates electromagnetic field peaks and nodes, i.e. optical lattice, which is similar to the crystal lattice. This creates semblance of crystal lattice in absence of actual medium. Furthermore, averaging interaction of a particle with both crystal and optical lattices one derives effective potential responsible for particle channeling in these systems. And this descriptive similarity is not the only reason for treating the considered process as channeling. However, on the contrary to crystal channeling when the channel cross-size is fixed within several nanometers, at laser channeling the channel size relates to the laser wavelength and the crossing angle of lasers. Thus, we deal with a large channel-size variation. Indeed, high current applications might be successfully realized for laser channeling on the contrary to crystal channeling due to the fact that the channels of cross-laser field might accept much more particles due to much larger channel width. Moreover, in case of laser field we do not care of inelastic scattering, which strongly influences at crystal channeling.

Another reason lies in the similarity of possible applications and effects found for optical and crystal lattices. The effective potentials of both crystal and optical lattices are similar, and both are capable of trapping electrons. So that channeled electron beams can be transported, focused and reflected by the potentials of both lattices. Bending a crystal one obtains a tool for charged particles beams steering, and bent laser channels might be also applied for this. Such bent laser channels might be formed by illuminating a curved reflecting surface with a laser at some angle that creates an interference region with the potential channels near the reflecting surface. Besides, the researches have recently shown different regimes of charged particles dynamics in presence of intense laser fields that are analogous to crystal volume reflection, to both planar and axial crystal channeling and optical undulating (Dik et al., 2018; Frolov et al., 2018).

2.3. Channeling in plasma-ion cavities

As known, interaction of intense ultrashort laser pulses in a medium can be used as a source of compact electron beams with successful its acceleration over short distances (Mangles et al., 2005). Due to the progress in laser technology (Mourou et al., 1998) the propagation of nonlinear electromagnetic waves in media became very interesting to be deeply investigated. Studies performed successfully has shown that powerful ultrashort laser pulses propagating in a plasma created by forward laser pulse can accelerate the plasma electrons to ultra-relativistic energies (Tajima and Dawson, 1979; Bulanov et al., 1990; Faure et al., 2004; Kostyukov et al., 2006).

Considering the problem of powerful ultrashort laser pulse interaction with a plasma based on numerical simulations, a model for a strongly nonlinear regime of interaction of intense laser pulses with plasmas has been earlier proposed. The model has demonstrated that in the process of laser interaction in media the plasma electrons are typically displaced by the laser pulse from the region of their localization. Heavy ions react to the laser impulse much weakly remaining “quasi-frozen” in a solid lattice. Hence, the laser propagation creates a cylindric channel characterized by electric field in transverse cross-section, which creates a potential well, and oriented longitudinal electric field as well. The longitudinal field propagates with a phase velocity close to the velocity of light. It accelerates electrons bound within the potential well that might be considered as a fast moving system. This process has been previously described within the phenomenology of “moving charged bubble” (see in the review (Esarey et al., 2009), Fig Fig 3). The bubble inside is free of electrons that makes it positively charged.

The moving bubble forms laser-pulse-oriented field gradient. It is transverse limited in a space defined by the laser cross-section. Simultaneously, for bound electrons this field becomes accelerating longitudinally. Thus, we can represent the interaction cavity as a plasma-ion channel, which is a distinct potential well for electrons (Dik and Dabagov, 2013; Dik et al., 2013). At definite conditions this potential traps the plasma electrons consistently accelerating them. In other words, acceleration of electrons in plasma-ion channels becomes easily described within the phenomenology of electrons channeling at presence of accelerating electric field.

Another very interesting phenomenon is widely known as “betatron radiation” of electrons accelerated by laser impulse in plasma channel. However, this type of radiation would be more correct to call “channeling radiation” in accelerating field. The reason for such declaration comes from the fact that the concentration of electrons close to the plasma channel axis appears because of known flux-peaking phenomenon (a kind of redistribution of the beam in a cylindric potential well),

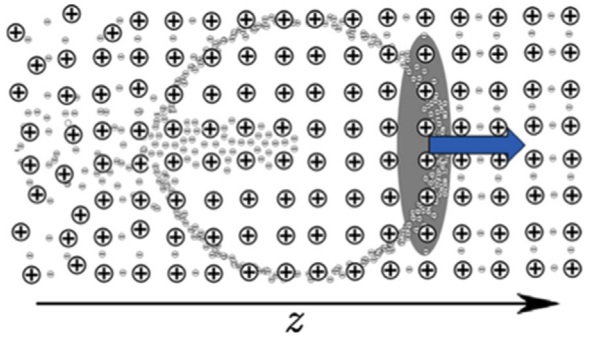

Fig. 3. Scheme for moving bubble that forms a channel for electron trapping and successful its acceleration.

a typical channeling feature, and not of the presence of stabilizing magnetic field.

2.4. Channeling in hollow guides

Manipulation of matter on the atomic scale will require new tools for lithography and metrology, and radiation at X-ray wavelengths will be fundamental to the development of this area. Progress within the fields of nanotechnology and X-ray propagation will be mutually beneficial. For instance, some types of processes based on the self-organization of materials that have recently attracted considerable interest because of the possibility of preparing fine patterns of nanometer dimensions over larger areas, can be used for the fabrication of X-ray waveguides (Spiller and Segmuller, 1974; Pogossian and Gall, 1995). X-ray propagation in nanochannels (Spiller and Segmuller, 1974) is important due to potential applications in X-ray optics. A special feature of these structures is a long, hollow, inner cavity, which could act as a channel for selective radiation penetration, similar to channeling of charged particles in crystals (see (Dabagov, 2003a) and Refs therein); nanochannels can be considered as capillaries (the basics of capillary/polycapillary optical elements (CO/polyCO) (Kumakhov and Komarov, 1990; Engström et al., 1991; Thiel et al., 1992)) (Fig. 4).

Research in X-ray propagation in capillary structures shows that diminishing the capillary internal radius from microns to nanometers results in a change of the character of radiation propagation, from the surface channeling in microcapillaries down to bulk channeling in nanocapillaries (Dabagov and Uberall, 2007, 2008) (Fig. 5). Bulk channeling describes the features of X-ray propagation in waveguides of various geometry and origin. Tapered waveguide optimization has been analyzed for getting high beam concentration by means of X-ray nanostructures (Panknin et al., 2008).

Numerical simulations (Zhevago and Glebov, 1998; Dedkov, 1998)

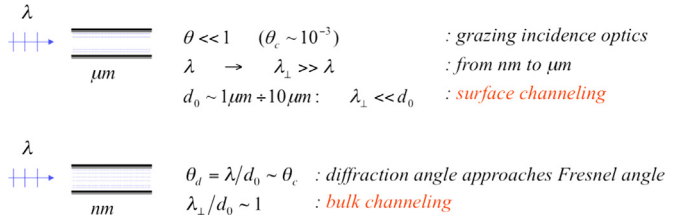

Fig. 5. Diminishing the channel size from microns to nanometers results in a change of the character of radiation propagation, from surface channeling in microchannels down to bulk channeling in nanochannels.

have shown that carbon nanotubes will act as soft X-ray waveguides and support modes of propagation when coated with various materials (Childs and O'Neill, 2003). The angular dependence of the intensity of characteristic K_α radiation in carbon versus aligned carbon nanotubes orientation suggests the possibility of X-ray channeling as well as radiation diffraction on nanotube multiwalls (Dabagov et al., 2003; Dabagov and Okotrub, 2004; Okotrub et al., 2005; Dabagov, 2011).

One should note that other researchers have already demonstrated experimentally the coherent propagation of X-rays in a planar waveguide with a tunable air gap (Zwanenburg et al., 1999, 2000) as well as the possibility of X-ray deflection over large angles being trapped by a curved X-ray waveguide (Salditt et al., 2015).

The modes of radiation propagation in a waveguide are revealed at interference between the incident and reflected waves forming a standing wave pattern (Spiller and Segmuller, 1974). However, it becomes constructive just for specific angles. This phenomenon, valid for reflection from a flat surface, takes place just in the vicinity of the surface. Similar phenomena might be observed at radiation reflection from a curved surface (so called “whispering modes”) (Vinogradov et al., 1985). Strong radiation redistribution also takes place behind capillary systems (which is actually a simple example of the curved surface system); some structural features in the distribution are due to the spatial geometry of a system (typically, hexagon type in the transverse cross section). However, some fine features could not be interpreted by ray optics, and require solution of the wave equation for radiation propagation.

A first theoretical note regarding the possibility to observe X-ray interference behind the system of capillaries with the channel diameter much over the radiation wavelength was published as an internal note (Dabagov, 1992). Then, the phenomenon was observed in a set of experiments on propagation os synchrotron radiation through polycapillary optical elements (channels sizes of ~ 100 μm, radiation wavelength ~ 1 ÷ 10 Å) (Dabagov et al., 1995a). The features recorded were interpreted within the wave propagation approach. The phenomenology of experimental pictures (Dabagov et al., 1995b) has shown that the fine features of X-ray propagation in micron-size

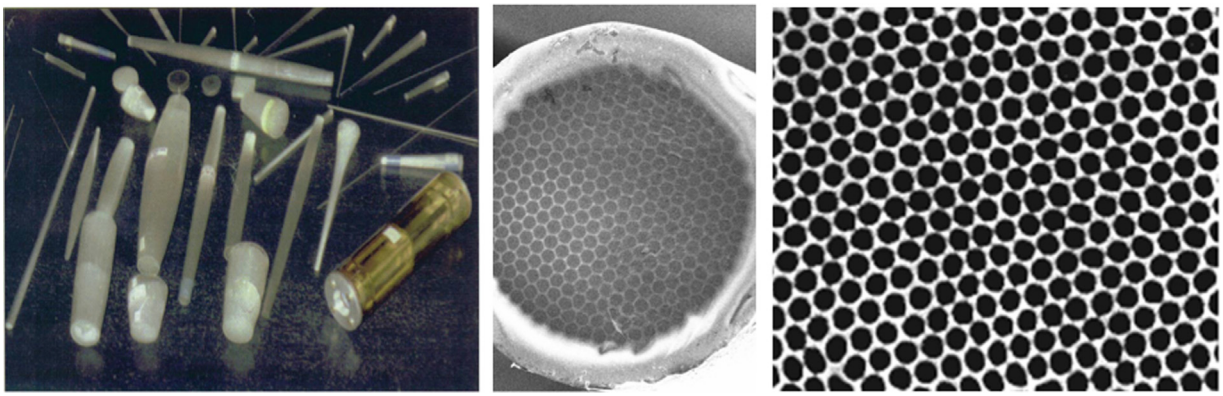

Fig. 4. Samples of polycapillary optical elements (left); transverse cross-section image of a single polycapillary (center); zoomed image of polycapillary cross-section (right).

channels can be explained in view of the radiation interference due to the various channel curvatures. Later the trapped radiation propagation in the very vicinity of 1d/2d curved surfaces was carefully studied in a number of papers (Dabagov and Kumakhov, 1995; Alexandrov et al., 1998; Artemiev et al., 1998; Dabagov et al., 2000, 1998; Liu and Golovchenko, 1997; Kukhlevsky et al., 2000; Cappuccio et al., 2001; Dabagov, 2003b) where the wave theory of X radiation propagation along a curved surface was developed (for complete citation, see Refs in (Dabagov, 2003a)). These features have been proved by other authors aforementioned.

3. X-Ray channeling

3.1. X-ray trapped propagation in micro- and nano-channels

The criterion to observe the wave features at propagation of radiation in the medium of length L is very simple. The transverse space where radiation is limited at propagation (independently on the medium, either a profiled surface or a specific collimation system) should be comparable in size with the transverse radiation wavelength $X_\perp \simeq \lambda_\perp$, where $\lambda_\perp \simeq \lambda/\vartheta_c$ with the critical angle for X-ray total external reflection ϑ_c. At radiation reflection from a flat surface as well as at its propagation in a planar waveguide the transverse dimension of a beam is estimated as $X_\perp \simeq L\vartheta_c$ getting a very simple and important relationship between radiation and optics parameters $L\vartheta_c^2 \simeq \lambda$. It allows the limits for revealing the wave features at reflection to be evaluated (Dabagov and Uberall, 2007). In case of curved planar or circular waveguides, taking into account that in approximation of glancing angles $\vartheta \ll 1$ one defines the longitudinal size of a curved reflecting surface $L \simeq r_{curv}\vartheta$ with the curvature radius r_{curv}, we reduce the expression $r_{curv}\vartheta_c^3 \simeq \lambda$ as the requirement to reveal wave features in multiple reflection optics (Dabagov et al., 1995b). For instance, it explains why even at nm wavelength radiation propagation in μ-channels the wave behaviors become observable.

Moreover, analysis of X radiation propagation through the guides of various sizes and shapes has shown that the character of radiation transmission is defined by the ratio of the transverse wavelength of radiation to the effective transverse size of a guide. That, in turn, is determined by the relationship between the diffraction and Fresnel angles, i.e. $\lambda_\perp/d \equiv \vartheta_d/\vartheta_c$. When this ratio is rather small, i.e. when the number of bound states is large, the ray optics approximation is valid. At $\lambda_\perp \simeq d$ a few modes are formed in a quantum well (a single mode for $\lambda_\perp \gg d$), and the wave theory must be applied. However, all these features can be described within an unified theory of X-ray channeling: surface channeling in μ-size guides and bulk channeling in n-size guides (Dabagov and Uberall, 2008).

The passage of X radiation through the guides is mainly defined by its interaction with the inner guide walls. In the ideal case, when the boundary between hollow channels and walls represents a smooth edge, the beam is split in two components: the mirror-reflected and refracted ones. The latter appears sharply suppressed in the case of total external reflection (TER). The characteristics of scattering inside the structures of ultra-small holes of various shapes might be evaluated from the solution of Helmholtz equation. In the first order approximation, propagation of X radiation through specially designed guides, the cladding material of which is characterized by the refractive index $n = 1 - \delta(\mathbf{r}) + i\beta(\mathbf{r})$ (the refraction δ and absorption β functions determine the guide geometry) is described by the wave propagation equation

$$(\boldsymbol{\Delta} + k^2 n^2(\mathbf{r}))E(\mathbf{r}) = 0, \quad n \equiv \begin{cases} 1 & , \ hollow\ core \\ n_0 = 1 - \delta_0 + i\beta_0 & , \ cladding \end{cases} \tag{1}$$

for the electromagnetic field amplitude E, where $\mathbf{k} \equiv (k_{||}, k_\perp)$ is the wave vector of radiation, $k = 2\pi/\lambda$, $\boldsymbol{\Delta} \equiv \partial^2/\partial\mathbf{r}_\perp^2 + \partial^2/\partial z^2$ is the Laplacian, $\mathbf{r} \equiv (\mathbf{r}_\perp, z)$. Presenting the radiation field as $E(\mathbf{r}) = E(\mathbf{r}_\perp)e^{ik_{||}z}$ and neglecting absorption ($|\delta| \ll 1$, $|\beta \ll |\delta|$), Eq. (1) is reduced to

$$[\boldsymbol{\Delta}_\perp - (2k^2\delta - k_\perp^2)]E(\mathbf{r}_\perp) = 0 \tag{2}$$

where the right side term in brackets is the potential of interaction V_{eff}. Due to the fact that the transverse wave vector under the grazing wave incidence $\vartheta \ll 1$ can be defined as $k_\perp \approx k\vartheta$, the effective interaction potential is estimated by the expression

$$V_{eff}(\mathbf{r}_\perp) = k^2(2\delta(\mathbf{r}_\perp) - \vartheta^2) = \begin{cases} -k^2\vartheta^2 & , \ guiding\ channel \\ k^2(2\delta_0 - \vartheta^2) & , \ cladding \end{cases} \tag{3}$$

From the latter the phenomenon of TER at $V_{eff} = 0$ follows when $\vartheta \equiv \vartheta_c \simeq \sqrt{2\delta_0}$. One can see that Eq. (2) corresponds to the Schrödinger equation for a particle of mass $k^2/2$ and kinetic energy ϑ^2. Hence, we can utilize the terminology of "channeling" where the channel is formed by the effective potential of radiation interaction in a guide (a quantum well).

Eq. (2) for radiation propagation in a medium with the potential Eq. (3) can be solved for the case of μ-guides as well as for n-guides. The principal difference of radiation propagation in μ- and n-channels is defined by the ratio between the effective guide-channel size and the transverse wavelength of radiation. The guiding channel is defined by its shape in μ-channels (collimation profile or surface curvature) whereas for n-channels - by the transverse channel size.

3.2. Basics for polycapillary optics

Let us estimate the effectiveness of a capillary system in controlling beams of X-ray radiation (note that our approach is valid not only for X-ray radiation but also for thermal and cold neutrons). Since the critical TER angle for X-rays is small, the angular aperture, acceptance, of a monocapillary (monoCO)[2] at its entrance is small, too

$$\Delta\varphi_m \propto \theta_c \ll 1 \tag{4}$$

This implies also a low transmitted power

$$W_m \propto \theta_c^2 \ T_m, \tag{5}$$

where T_m is the transmission coefficient defined by the monoCO parameters as well as the quality of its inner reflecting surface. In the case of a conical focusing monoCO the gain in radiation power of three or more orders of magnitude can be achieved at its exit (Fig. 6a). Such optics is difficult to be fabricated from the technical viewpoint. They are very long, several tens of cm, and effective only in the case of a quasi parallel radiation source of small transverse dimensions (in particular, for the 3rd generation synchrotron radiation sources).

The efficiency of such systems can be increased by using polycapillary systems (polyCO) (Fig. 6b). PolyCO represents a bundle of thousands single capillaries merged in one system. It is characterized by many channels in cross section that has been shaped, utilizing a special technology, to have one focus. Additional technical manipulations allows us to get various-shape polyCO systems. Obviously, the entrance angular aperture of a polyCO might be much larger than the critical TER angle,

$$\Delta\varphi_p \gg \theta_c, \tag{6}$$

that results in the essential increase of the transmitted radiation power according to the expression

$$W_p \propto (\Delta\varphi_p)^2 \ T_p \gg W_m \tag{7}$$

Here T_p is the transmission coefficient of polyCO, and we assume that the transmission through the system is not low ($T_p \geq 10\%$). A specially designed polyCO enables not only for effective radiation transmission but also for the increase of the radiation density $w \simeq W \ / \ (\Delta f)^2$ by focusing the radiation into a small-size spot Δf. Hence, such a capillary system can

[2] A monocapillary optics (monoCO) represents a single capillary; in literature it is mostly known as capillary optics (CO).

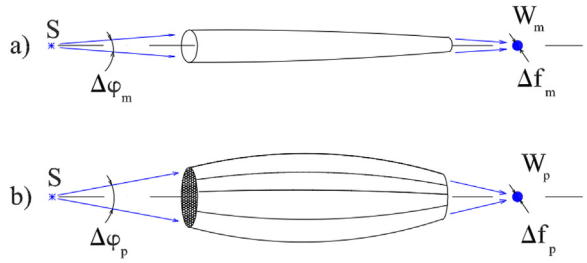

Fig. 6. Scheme for comparison of mono- and polyCO (reproduced from Dabagov, 2003).

operate as a focusing lens.

Let us examine a capillary lens with an angular aperture $\Delta\varphi_p$. If the transmission of the lens is T_p, the power of the radiation focused to a spot of diameter Δf_p obeys the following expression

$$w_p \propto \pi\left(\frac{\Delta\varphi_p}{2}\right)^2 \frac{T_p}{(\Delta f_p)^2} \tag{8}$$

Since the radiation density at a distance L from the source inversely proportional to the distance, $w_0(L) \propto 1/(4\pi L^2)$, the use of a capillary lens allows achieving the following gain in radiation density

$$G \equiv \left(\frac{w_p}{w_0}\right)_L = \left(\frac{L\Delta\varphi_p}{\Delta f_p}\right)^2 T_p \tag{9}$$

The gain G determines the effective distance from the source of radiation at which radiation density without optics is equal to the radiation density at the focal spot of the capillary lens, i.e., $w_0(L_{eff}) = w_p(L)$. This yields the following convenient expression for calculating the efficiency of the optics

$$L_{eff} = \frac{L}{\sqrt{G}} = \frac{\Delta f_p}{\Delta\varphi_p\sqrt{T_p}} \tag{10}$$

Here, L_{eff} is the effective focusing length, which determines the distance by which the irradiated object is 'moved' closer to the radiation source. For instance, if the radiation density gain at the lens focus is 100, the effective proximity of the focus to the source decreases by a factor of 10. On the other hand, if we reduce the effective distance by a factor of ~ 3 by varying the parameters $\Delta\varphi_p$, $\Delta f_p T_p$, the radiation density in the focal plane of the capillary system might be increased by a factor 10^3.

These simple estimates help us to understand the polyCO potential to increase the radiation flux on a sample. Similar estimations allow evaluating the ability of beam shaping (especially getting a quasi parallel beam) by means of so-called polyCO semilens (half-lens) that also proves the possibility of getting high-flux quasi parallel X-ray radiation.

3.3. Polycapillary based X-ray spectroscopy and imaging

As known based on X-ray channeling inside hollow tubes polyCO technology has been developed since the middle of 1980 s. PolyCO presently is one of the most powerful X-ray instrument to handle X-ray beams (shaping and focusing). The optics has shown high efficiency once applied in optimized X-ray experiments (Hampai et al., 2008, 2009, 2011, 2013a, 2013b, 2015, 2017; Allocca et al., 2010; Marchitto et al., 2013, 2015; Polese et al., 2014; Liedl et al., 2015; Bonfigli et al., 2016; Cherepennikov et al., 2017). For instance, one should underline a high potentiality in applications for X-ray fluorescence and diffraction analyses, for X-ray imaging, etc. A special confocal scheme for micro X-ray fluorescence measurements that enables obtaining not only elemental mapping of a sample but also simultaneously its X-ray image has been proposed and realized. The prototype of a compact X-ray spectrometer characterized by a spatial resolution of less than 100 μm for fluorescence and less than 10 μm for imaging has been designed. New results on submicron spatial resolution for X-ray imaging by a table-top laboratory system based on lithium fluoride (LiF) imaging radiation detectors and X-ray tube combined with polycapillary optics has been reported for the first time. Recently a new technique for fast tomography of low absorbing samples (organic samples, sprays, etc.) by means of the optimized combination of conventional X-ray tube, polycapillary optics and synchronization system has been developed. Let's analyze our selected results on the use of polyCO samples for various X-ray techniques presented below.

In order to test the ability of the optics to increase the radiation flux a polyCO lens optimized for the Mo K_α line (17 keV, nominal transmission 35%) is selected. Its geometrical parameters are characterized by the cross-sections at the entrance, maximum and exit as follows: $D_{ent} = 5.2$ mm, $D_{max} = 6.8$ mm, $D_{ext} = 4.6$ mm, the lens length $L = 111.5$ mm and the channel internal diameter d $\sim 8\,\mu$ m. The size of the input spot collected by the lens, for the energy of our interest (25 keV), is estimated to be 149.61 μm, which for the alignment procedure is conveniently smaller than the focal spot on the tube anode. The TER critical angle θ_c for X-ray photons of 25 keV is ~ 1.2 mrad, equivalent to 0.069°. The lens has been experimentally characterized as regards its input/output focal distances and spot size, respectively, resulted to be $\sim$ 65/43 mm and $\sim$ 145.6 μm. With this geometry, the solid angle captured by the lens is 5.4×10^{-3} sr, while a pinhole collimating the same spot size at the same distance collects a solid angle of 3.8×10^{-7} sr. Thus, the solid angle and the lens nominal transmission efficiency as defined in Eq. (9) should result in a gain factor of $\sim 10^2 \div 10^3$ for various spectrum frequencies.

To experimentally verify also the gain factor in the excited fluorescence signal with respect to the use of a pinhole, two XRF (X-ray fluorescence) spectra of a reference glass sample have been recorded by a SDD detector (Silicon Drift Detector) with active area of 30 mm^2. The acquisition time was 120 s, and the W anode tube was set at 50 kV and 500 μ A. For both configurations, polyCO or pinhole based, the sample was placed at the same distance from the source. Fig. 7 shows the comparison between two XRF spectra. The better excitation provided by the lens, which allows detecting the elements otherwise not visible with the pinhole, is evident. The polyCO sample, being designed for low X-ray frequencies ($\sim 3 \div 10$ keV), provides an excitation gain of 3 orders of magnitude on Ti K_α (4.5 keV) and of 2 orders on Mo K_α (17 keV).

A number of imaging experiments using polyCO lenses has been performed recently proving the feasibility of the polyCO use for X-ray imaging that is characterized by the improved experiment and image parameters with respect to typical X-ray imaging techniques. In our recent studies we have confirmed the possibility to develop a desktop device combining X-ray tube and polyCO for imaging of organic materials. A key physical parameter to be utilized is the beam blurring, which is strongly related to the radiation divergence in front of the sample and behind it as well.

Hence, to obtain a rather small radiation divergence a polyCO semilens was used that allowed getting a very small blurring effect. Since the used semilens has a residual divergence of 1.5 mrad, and the sample can be placed about 15 mm from the detector due to the physical dimensions of the stage rotation, our minimum resolution can be estimated about 15 μm, which is comparable to the CCD (Charge Coupled Device) resolution. For X-ray imaging, as well as successfully for tomography, we have utilized, as a radiation source, an Oxford Apogee 5000 tube (Cu K_α) with a source spot of about $50 \times 50\,\mu m^2$ and power of 50 W, a Photonic Science CCD FDI 1:1.61 (FDI is a high resolution, high speed, digital imaging camera) with a pixel resolution of $10.4 \times 10.4\,\mu m^2$ and a Newport micrometer used for optimized $xyz\theta$ positioning.

One of the most impressive imaging experiment can be recognized as a 3D image reconstruction experiment carried out using an organic sample, namely, a piece of lifeless ant. The examined sample is positioned on a $xyz\theta$ micro-positioner and rotated by 0.5° per image, for a total of 720 projection images. The rotation velocity of 0.5°/s, then the entire scan time of 720 s was chosen to get optimized data for further

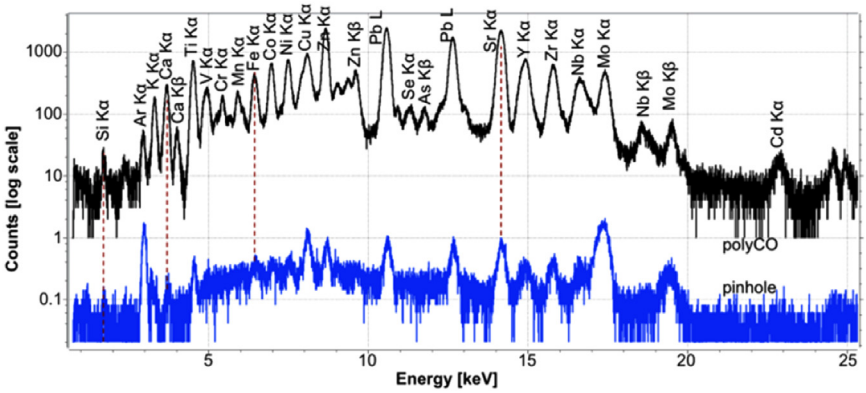

Fig. 7. XRF spectra obtained using a pinhole (lower, blue curve) and a polyCO (upper, black curve).

image processing. The short exposition time was 250 ms keeping the CCD non-saturated. As a pre-processing, each image is treated with the CCD image program "Image-Pro Express" that allowed removing the background noises. The further reconstruction work to convert projection images into slice images has been done with the OCTOPUS code (www.inct.be,), and successfully the rendering work was carried out with the AMIRA code (www.amira.com,). Fig. 8, left shows the 3D rendering of an ant (side view) from the reconstructed slice images. A second rendering was carried out by highlighting the inner parts with well-recognized structures of the central nervous system and the mandibular glands (yellow-brown areas) (Fig. 8, right - the picture taken from the bottom of an ant).

The CT images obtained by the laboratory facility based on the use of polyCO have shown essentially high efficiency of polyCO based desktop scheme for getting high-resolution X-ray images. The image qualities are comparable with those obtained at synchrotron radiation facilities.

The second imaging mode for organic media examined within dedicated collaboration is the tomography of a fast dynamical process in air, i.e. in our case it was a spray emitted by a fuel injector of the car engine. As known tomographic investigation of such process might be performed using powerful synchrotron-radiation sources because of: a) the low absorbance of the fuel that results in a very low contrast with the surrounding air, and b) the speed of the spray dynamics, of the order of milliseconds. Indeed, a weak image signal variation in the spray spatial distribution requires an intensity/divergency optimized flux from the source to achieve a sufficient signal-to-noise ratio.

Actually, in this case the flux density enhancement by polyCO might enable the use of conventional X-ray source. A dedicated experimental box with a rotating system and a trigger acquisition chain was assembled, while, in order to increase the absorption, a small quantity of additive containing a high Z element (cerium) is added to the fuel. The polyCO semilens coupled with the X-ray tube generates a quasi parallel beam inside the experimental box. Projections are collected on the opposite side of the box using a CCD camera (10.4 μm of pixel size). The tomography is performed covering 180°, collecting images every 1° rotating around the axis centered on the injector tip. An electronic signal triggered the injection event at 4 ms. The injection process is split into three steps: a first phase, in which the fuel flux grows, a second stationary with a stable fuel flux, and a third final phase when the flow decreases ending the injection. Hence, the image acquisition is triggered with a delay of 500 μs respect to the injection start and a duration of 3 ms. In this way the X-ray projection is referred to the stationary interval of the injection. For each angular position the acquisition is repeated 100 times. The average of these images results in an enhanced signal to noise ratio image. Each averaged image is taken as a projection of the spray. In Fig. 9 the 3D rendering of a spray that results composed by six distinct jets is shown. Starting from the grey values of the reconstructed images, it is possible to extract the density distribution of the fuel inside the spray. A pseudocolor scale has been applied spreading from the blue for lower absorption intensity to red for maximum. The field of view of the object is limited to the part immediately downstream the nozzle tip, sizing about 3 mm. Two views of the jets are reported: on the left - a side view, corresponding to the camera field of view, while on the right - a top side from the nozzle location.

Apart of getting high-resolution CT images of developing sprays shown here, the technique proposed allows also deep analysis of the spray jets evolution revealing fine features of the fuel dynamics in real engines.

To demonstrate the possibility for recognizing the nanostructures, the imaging experiments might be performed combining polyCO with a high-resolution detector, for instance, constituted by a lithium fluoride (LiF) crystal. Indeed, LiF crystals have a particular sensibility to ionizing radiation making them suitable as X-ray detectors with a theoretical resolution close to the atomic scale. The interaction between X-rays and LiF crystal lattice creates stable electronic defects at room temperature. The size of these defects known as color centers defines the theoretical spatial resolution of an image collected irradiating a LiF crystal. Defects created by a X-ray beam have a characteristic absorption band around 450 nm and can be excited with a visible light in the blue spectral range. The illumination induces a consequent photoluminescence effect from defects within green and red spectral ranges. In this way, after the X-ray illumination, using a Confocal Laser Scanning, or a Scanning near field optical microscope, the defects created by irradiation can be detected using their photoluminescence. The response is proportional to the incident X-ray power released during the irradiation. The technique is then sensitive to the projection absorption pattern when a sample is just left on top of a LiF crystal. The main drawback of this layout is the low efficiency of the irradiation-defect creation process. Actually, several hours are needed to collect a single

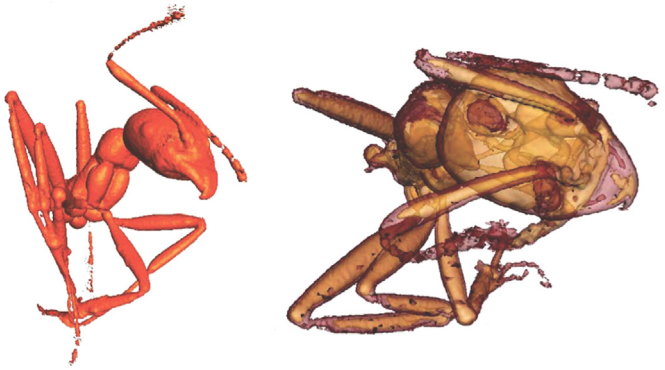

Fig. 8. CT for an ant by polyCO. Rendered image of an ant after reconstruction. The mandible, the eye and the arms are well seen (left). Rendered image of an ant: the yellow-brown areas represents the inner structures of the sample, such as the nervous system (right).

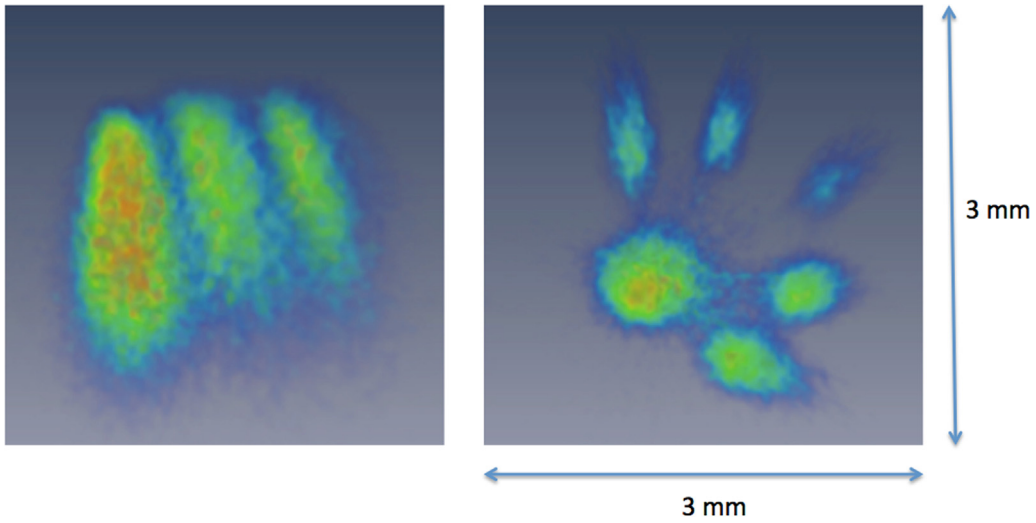

Fig. 9. Spray Image by polyCO. Tomography pictures of the six-hole GDI spray: side view (left) and top view (right).

image and just for this reason, the enhanced flux density due to polyCO has been considered to perform faster imaging. In the tests a semilens is used to provide the beam: a high radiation flux on a circular beam section of 3 mm of diameter.

For these tests, the experimental layout is composed by an X-ray tube coupled to a polyCO semilens. The sample and the detector are set on the optical axis of the beam transmitted by the semilens in order to project the absorption pattern on the LiF detector. A first test was performed with an Au grid, 1000 line/inch, constituted by wires of 6 μm of diameter spaced by 19 μm. The sample was placed closest as possible to the detector, a $5 \times 5 \times 0.5\,mm^3$ LiF crystal (Fig 10). In Fig. 10 the analysis of Au grid test also compared with its projection recorded by a CCD camera with a 3.5 μm pixel size. The LiF image shows not only a better resolution compared to the CCD image, but well reproduces the size of the wires. As shown by the line profile (Fig. 10d) the projected image of a wire is ~ 6.5 μm width.

The experiment with a LiF detector was also performed on a cordierite slice with the composition $(Mg,\ Fe)_2Al_4Si_5O_{18x}(H_2O,\ CO_2)$ coming from the granite enclave within the dacitic lava dome of El Hoyazo. The crystal was a doubly polished (010) section with thickness of 140 μm. In Fig. 11 the optical and X-ray projection are compared. In Fig. 11b various internal features of the sample are detected, while in Figs. 11c and 11d the intensity profile along two profiles (direction L and L of Fig. 11b) are shown. Both curves demonstrate very high spatial resolution of this imaging technique.

Recently, a new experimental layout, the “Rainbow X-Ray” (RXR) station, has been designed and installed at XLab Frascati of the Frascati National Laboratories (XlabF LNF). RXR is a rather compact experimental apparatus dedicated to 2D/3D X-ray micro-fluorescence (μ XRF) spectroscopy. Its main parameters are a probe size ranging between 70 and 80 μm and an excitation energy from 0.8 to 30 keV. This setup allows us to work with different experimental layouts including the one for total reflection XRF analysis (TXRF) to detect low concentration elements. The RXR layout is based on a confocal geometry design that allows performing the elemental depth profiling for different types of samples. The “confocal” approach simplifies the measurement procedure and enables discriminating depth-dependent signals from high to low Z elements. Moreover, it avoids the negative superposition of images (Hampai et al., 2018).

The RXR setup is composed by three dedicated polyCO elements. A polyCO lens focuses the incident beam to the sample position, while two semilenses, one optimized for low energy (0.8 ÷ 6 keV) and a second one for high energy (6 ÷ 30 keV), concentrate the fluorescent radiation to the detectors. The use of two different semilenses enables us to carry out measurements both in air for the high Z elements (Z > 15) and in vacuum for low Z elements (Z > 8). Additionally, due to the possibility to collect 3D micrometrical scans our experimental layout can perform the 3D tomography of a sample in a wide energy range, from 1 up to 30 keV.

Compared to tomography, the 3D μ XRF technique allows the recognition of specific elemental contributions. Again, as an example, in Fig. 12 a 3D rendering with the iron contribution outlined in red (b), the external surface of scattered beam (yellow) and the internal surface of the sample (grey) is showed. This “elemental” visualization, with a spatial resolution of ~ 100 μm, clearly highlights the presence of bubbles (see white arrows “a” of Fig. 12) formed in the hardening process of the glue.

3.4. X-ray channeling in microchannel plates

The theory for X-ray channeling in capillaries has been applied to X-ray propagation into microchannel plates that allowed clear explanation of experimental features for both X-ray propagation and fluorescent radiation distribution behind MCP samples (Mazuritskiy et al., 2013, 2014, 2015, 2016, 2017) (Fig. 13).

MCPs are the $SiO_2 - PbO$ glass systems consisting of a huge number ($10^4 \div 10^7$) of densely located straight parallel hollow channels normal to the MCP surface, regularly separated and of hexagonal symmetry in the transverse cross-section. Modern technologies allow creating MCP samples with very small channel sizes ($\sim 3 \div 5\,\mu m$) and distances between them ($\sim 4 \div 5\,\mu$ m). Since these dimensions are comparable to the typical dimensions of X-ray polycapillary optics, MCP itself can be considered as an optical element for X-ray frequencies. Since all channels are parallel to each other, it can be assumed that such a system might be effective as either a collimator or a radiation deflector, with the possibility of MCP use for X-rays focusing, too (Chapman et al., 1990, 1993; Kaaret et al., 1992; Brunton et al., 1997).

When the MCP is irradiated with a parallel flux of X-ray quanta at different angles, it is obvious that the channels of a flat MCP work the same way, the difference is only in the spatial coordinates of the radiation hitting the detector from a single capillary. However, if you bend such a system, the MCP becomes a focusing optical device (Fig. 14).

To prove the focusing peculiarities of a bent MCP, a metal wire might be used as an object for irradiation by the MCP transmitted beam. If originally parallel beam before MCP becomes indeed focused behind MCP, transformed in such a way in a convergent one, the shadow of metal wire (its X-ray image) should reveal well defined decrease in its

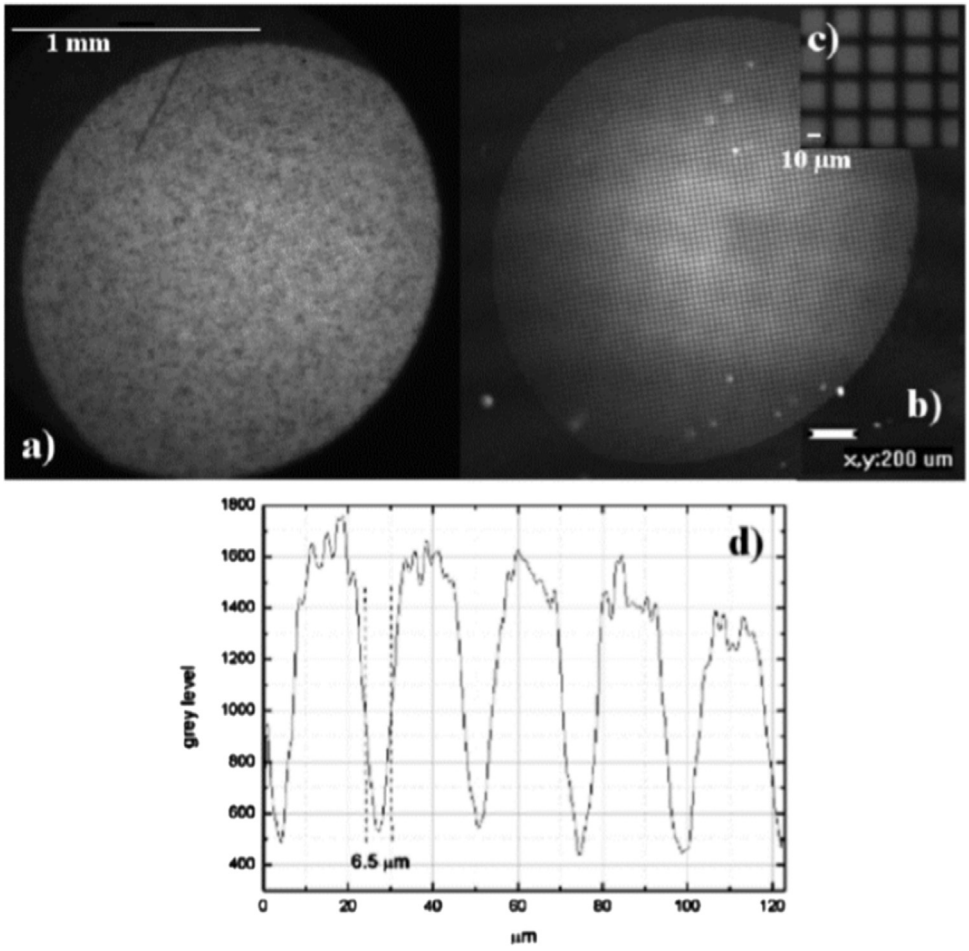

Fig. 10. Comparison of the Au grid radiographies recorded by CCD camera and LiF crystal. a) CCD: 3.5 μm pixel size b) LiF image read by a confocal microscope c) details of the LiF images d) plot of the LiF image line profile.

width on the screen (CCD). In the course of the experiment, a weakly curved MCP (with the curvature radius of R = 2 m) was irradiated by the flux at X-ray frequency range corresponding to Cu K_{α}. Behind the MCP, the radiation becomes convergent and hit the metal wire positioned at the longitudinal axis of the flux. At different positions of the detection screen relative to the optical system, the focusing properties of the curved MCP have been studied. We observe that the image of the wire gradually disappears when the screen approaches the bent MCP geometrical focus. This fact indicates that a parallel beam formed by a polyCO semilens and incident on the MCP is focused following the rotation of certain channels at MCP bending. The blurring of the wire contours, and then its disappearance at all moving the screen down to a value of the bending radius of the MCP.

The focusing features, however, can be explained in some specific cases within the formalism of single reflections of radiation in various MCP channels. Corresponding studies performed earlier by other authors have revealed the limits of MCP use to focus X-ray radiation. The restrictions were mostly related to the technology of MCP fabrication for past time.

Nowadays, with advanced MCP technology we can deal with much bigger ratio of the channel length to its width that makes MCP samples rather similar to polyCO ones. This fact is confirmed by the results of X-ray propagation through the MCPs of last generations. Recent studies have proved the fact that MCPs could act as X-ray optical elements. As confirmation, we present one of the results on X-ray transmission by MCP (Fig. 15)

The pattern of transmitted by MCP radiation has been calculated using a model of the diffraction process at the radiation far field. The MCP channels at the exit are considered as a multiple sources of radiation, the profiles of which are formed at multiple glancing reflections of radiation from the inner surfaces of MCP channels. Description of radiation propagation inside MCP channels is done by applying the channeling formalism. The comparison of theoretical and experimental distributions are in good agreement that proves the ability of MCP to act as a diffractive X-ray unit.

4. Resume

As shown in this report, generally saying, channeling phenomenology might be applied for any kind of charged or neutral particle beams motion in the external fields defined by long transversely limited channels (Dabagov, 2018). Moreover, various features of the structure as a periodic structure, for instance, may supply additional peculiarities of beam passing through such structures.

Channeling of charged particles in periodic crystals (monocrystals, complex crystals, nanostructures, etc.) has the potential to handle the beams: bent crystal channeling may result in beam steering at accelerators providing in such way the opportunity for beam extraction or collimation; at channeling the crystal can act as rather effective compact undulator; channeling becomes very promising instrument for cooling and accelerating muons, for production of positron, etc (Dik et al., 2016; Babaev and Dabagov, 2017; Dabagov and Kalashnikov, 2017; Abdrashitov et al., 2017; Maksyuta et al., 2017; Frolov et al., 2017).

Propagation of charged particles in crystals and propagation of photons/neutrons in capillary systems, even if strongly different by

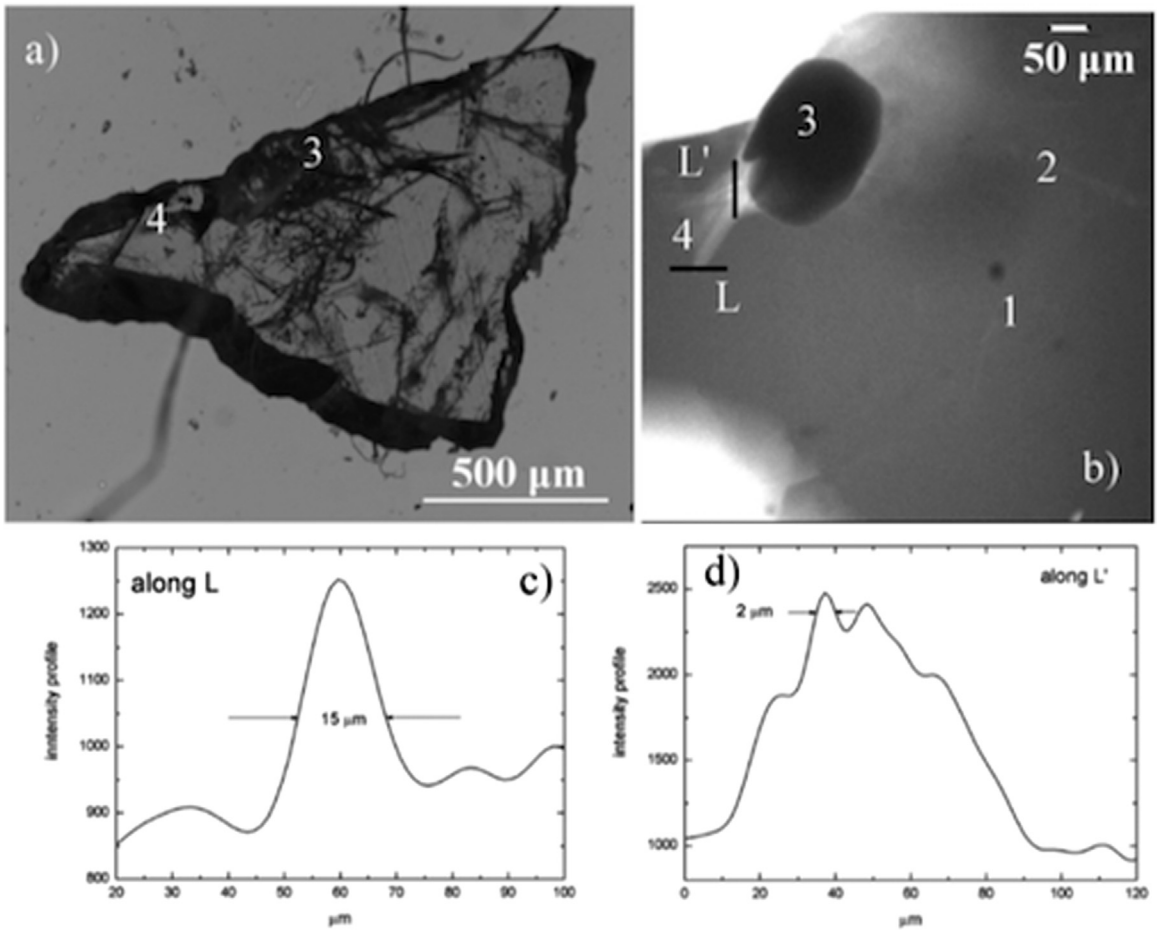

Fig. 11. Studies on an cordierite sample. a) Optical image in a transmission mode b) LiF image read by a confocal microscope c) and d) are the plot line profiles relative to L and L' lines. FWHM (full width at half maximum) of the brighter part was calculated.

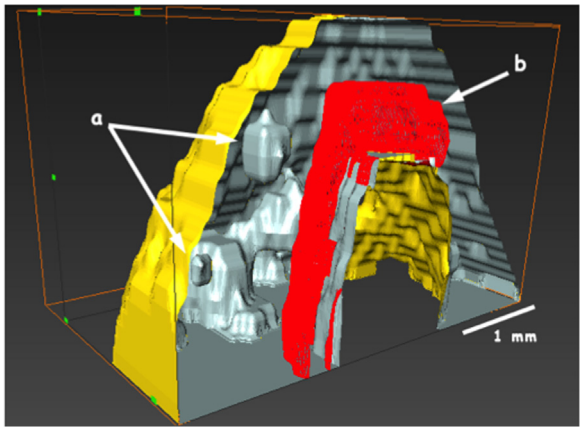

Fig. 12. 3D color XRF Image by polyCO. 3D reconstruction section of the screw encapsulated in the glue. The arrows a) and b) identify two air bubbles trapped during the hardening process of the glue [?].

nature, have much in common, i.e. both can be described within the frame of channeling theory. It works as useful method to control X-ray and gamma radiations for efficient beams deflection over large angles at very short distances allowing in such a way the radiation intensity of existing sources to be increased in orders of the value (capillary/poly-capillary optics, X-ray waveguides). Capillary optical systems are very powerful instrument to handle also thermal neutrons (Kumakhov and Sharov, 1992); manufactured by special technology capillary optical elements can transport large-aperture thermal neutron beams

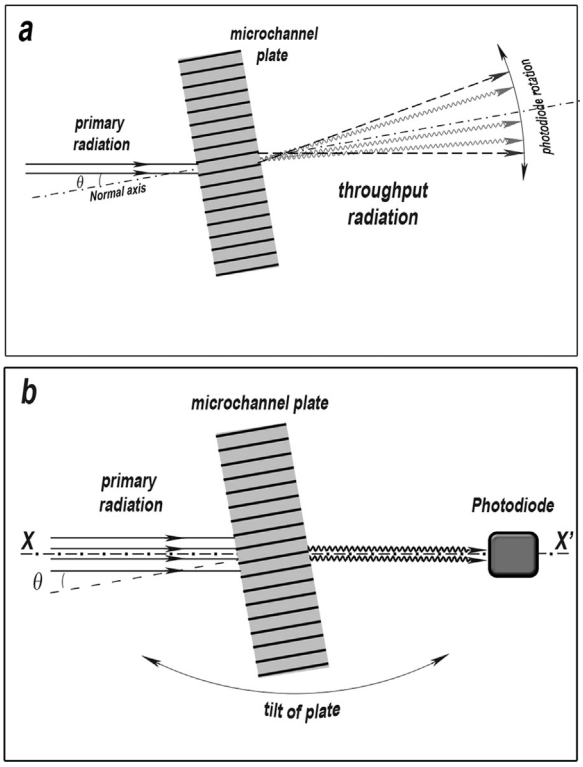

Fig. 13. Schemes for experiments on soft X-ray transmission by flat MCP.

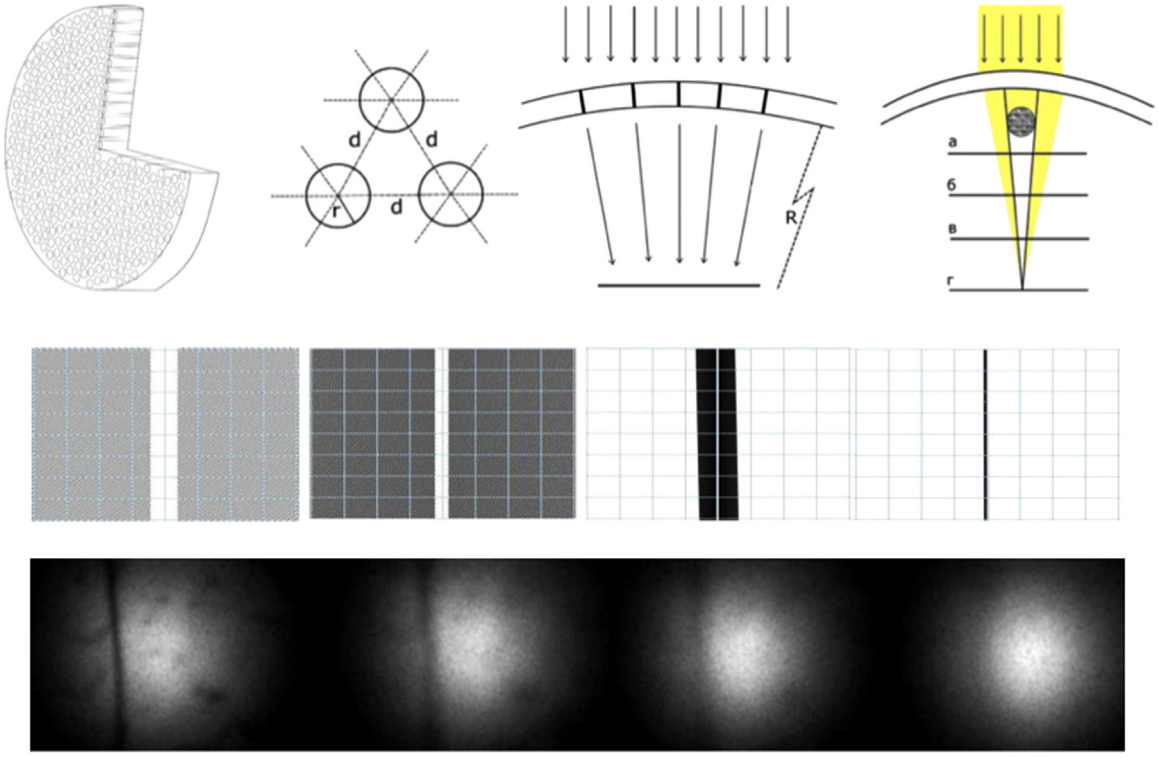

Fig. 14. Scheme for beam focusing by means of bent MCP. As explained by the scheme (upper picture) and proved by calculations (middle picture), a metal wire X-ray image disappears within convergent X-ray beam behind focusing MCP (lower picture).

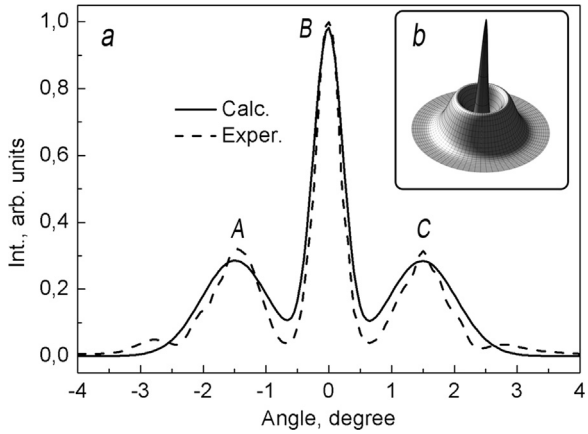

Fig. 15. Simulated (bold) and experimental (dashed) spectra of soft X-ray radiation transmitted by MCP as a function of the angle between incident radiation and longitudinal axes of the MCP channels.

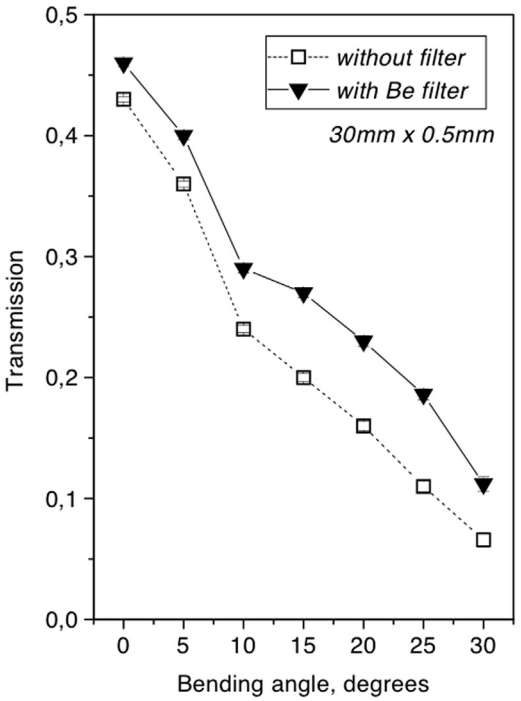

Fig. 16. Thermal neutrons deflection by polycapillary bender.

effectively bending them over the large angles (up to (25° – 30°)) in very limited space (~ 15 cm) (Ioffe et al., 1995; Dabagov et al., 2000) (Fig. 16).

Finally, it is worthy to underline that phenomenology of beams channeling attracts attention of various groups of researchers that is clearly reflected by the growing number of international meetings with corresponding topics.

Within the framework of our brief review, it was difficult to cover the whole spectrum of studies conducted in the world using the phenomenology of channeling. In particular, this concerns the use of capillary/polycapillary structures as optical elements for X-ray and neutron beams. The analysis given in the work was based on the results of our group, and, therefore, we do not claim the completeness of references on this topic. The aim of this work was just to highlight the main directions of the research on the use of channeling phenomena for various beams as it was presented at the International Forum on Advances in Radiation Physics - FORUMBA-2017 (Buenos Aires, May 2017).

Acknowledgements

The results presented in this short review are mostly based on the studies performed at the XLab Frascati LNF INFN (Frascati), the P.N.

Lebedev Physical Institute of the Russian Academy of Sciences (Moscow) and the National Research Nuclear University MEPhI (Moscow).

We are pleased to thank the organizers of the FORUMBA-2017 meeting, and personally its chairman Professor Jorge Fernandez, for the invitation to present the results of our studies on the use of channeling phenomenon. We would like to acknowledge the work done by our colleagues Augusto Marcelli, Dariush Hampai, Mikhail Mazuritsky, Katarzyna Dziedzic-Kocurek, Claudia Polese, Andrea Liedl, Luigi Allocca, Luca Marchitto, Alexander Baryshnikov and other colleagues contributed in our common researches.

SD recognizes the support by the Competitiveness Program of the NR Nuclear University MEPhI, Russia.

References

〈http://www.amira.com〉.
〈http://www.inct.be/en/software/octopus〉.
Abdrashitov, S.V., Bogdanov, O.V., Dabagov, S.B., Pivovarov, Y.L., Tukhfatullin, T.A., 2017. Total yield and spectra of positrons produced by channeling radiation from 0.1 ÷ 1.6 GeV electrons. Nucl. Instrum. Methods B 402, 54–57. http://dx.doi.org/10.1016/j.nimb.2017.03.105.
Akhiezer, A., Shul'ga, N., 1996. High-Energy Electrodynamics in Matter. G. & B. Sci. Pub., Amsterdam.
Alexandrov, Y., Dabagov, S., Kumakhov, M., Murashova, V., Fedin, D., Fedorchuk, R., Yakimenko, M., 1998. Peculiarities of photon transmission through capillary systems. Nucl. Instrum. Methods B 134 (2), 174–180. http://dx.doi.org/10.1016/S0168-583X(98)00554-0.
Allocca, L., Marchitto, L., Alfuso, S., Hampai, D., Cappuccio, G., Dabagov, S.B., 2010. Gasoline spray imaging by polycapillary X-ray technique, AIP Conference Proceedings 1221 (1) 191-195. 〈http://dx.doi.org/10.1063/1.3399248〉.
Andreev, A.V., Akhmanov, S.A., 1991. Channeling, collimation, and radiation of relativistic electrons in ultrastrong nonuniform optical fields. Zh. Eksp. Teor. Fiz. Pis'ma Red. 53 (1), 18–21.
Andriyash, I.A., Balcou, P., Tikhonchuk, V.T., 2011. Collective properties of a relativistic electron beam injected into a high intensity optical lattice. Eur. Phys. J. D 65 (3), 533–540. http://dx.doi.org/10.1140/epjd/e2011-20254-5.
Andriyash, I.A., d'Humières, E., Tikhonchuk, V.T., Balcou, P., 2012. X-ray amplification from a Raman free-electron laser. Phys. Rev. Lett. 109, 244802. http://dx.doi.org/10.1103/PhysRevLett.109.244802.
Andriyash, I.A., d'Humières, E., Tikhonchuk, V.T., Balcou, P., 2013. X-ray emission from relativistic electrons in a transverse high intensity optical lattice, J. Phys.: Conf. Ser. 414 (1) 012008. 〈http://dx.doi.org/10.1088/1742-6596/414/1/012008〉.
Appleton, B.R., Erginsoy, C., Gibson, W.M., 1967. Channeling effects in the energy loss of 3-11-MeV protons in silicon and germanium single crystals. Phys. Rev. 161, 330–349. http://dx.doi.org/10.1103/PhysRev.161.330.
Artemiev, N., Artemiev, A., Kohn, V., Smolyakov, N., 1998. Coherent phenomenon in reflection of radiation by an uneven mirror. Phys. Scr. 57 (2), 228.
Babaev, A., Dabagov, S., 2011. Angular distributions of bent-crystal deflected protons. Il Nuovo Cim. C 34 (4), 417–423.
Babaev, A., Dabagov, S.B., 2012. Simulations of planar channeling of relativistic nuclei in a bent crystal. Eur. Phys. J. Plus 127 (6), 62. http://dx.doi.org/10.1140/epjp/i2012-12062-6.
Babaev, A., Cavoto, G., Dabagov, S.B., 2013. Theloss of ions at beam multiple passage through a bent crystal. Nucl. Instrum. Methods B 309, 120–123. http://dx.doi.org/10.1016/j.nimb.2013.02.018.
Babaev, A., Cavoto, G., Dabagov, S.B., 2015a. Deflection of positively charged heavy particles by the crystal miscut surface. Nucl. Instrum. Methods B 355, 356–359. http://dx.doi.org/10.1016/j.nimb.2015.01.018.
Babaev, A.A., Cavoto, G., Dabagov, S.B., 2015b. On the deflection of a positron beam by the miscut surface of an oriented crystal. JETP Lett. 100 (9), 550–554. http://dx.doi.org/10.1134/S0021364014210036.
Babaev, A.A., Dabagov, S.B., 2017. Muon beam channeling in a laser standing wave. Nucl. Instrum. Methods B 402, 223–227. http://dx.doi.org/10.1016/j.nimb.2017.03.122.
Babaev, A., Dabagov, S.B., 2012. Inelastic nuclear interactions at protons multiple passage in bent crystals. J. Phys.: Conf. Ser. 357, 012032.
Baier, V.N., Katkov, V.M., Strakhovenko, V.M., 1998. High Energy Electromagnetic Processes in Oriented Single Crystals. World Scientific, Singapore.
Balcou, P., 2010. Proposal for a Raman x-ray free electron laser. Eur. Phys. J. D 59 (3), 525–537. http://dx.doi.org/10.1140/epjd/e2010-00185-5.
Baryshevsky, V.G., 1982. Channeling, Radiation and Reactions in Crystals at High Energies, BSU, Minsk, (in Russian).
Bazylev, V.A., Zhevago, N.K., 1987. Radiation of Fast Particles in Matter and External Fields. Nauka, Moscow (in Russian).
Beeler, J.R., Besco, D.G., 1963. Range and damage effects of tunnel tragectories in a wurtzite structure. J. Appl. Phys. 34 (9), 2873–2878.
Beloshitsky, V.V., Komarov, F.F., 1982. Electromagnetic radiation of relativistic channeling particles (the kumakhov effect). Phys. Rep. 93 (3), 117–197.
Bertolotti, M., Sibilia, C., Fuli, L., 1986. Channeling of Relativistic Electrons In A Periodic EM Potential. Springer Berlin Heidelberg, pp. 155–159. http://dx.doi.org/10.1007/978-3-662-10624-2_12.
Biryukov, V.M., Chesnokov, Y.A., Kotov, V.I., 1997. Crystal Channeling and Its Application at High-Energy Accelerators. Springer, Berlin.
Bonfigli, F., Hampai, D., Dabagov, S.B., Montereali, R.M., 2016. Characterization of X-ray polycapillary optics by LiF crystal radiation detectors through confocal fluorescence microscopy. Opt. Mater. 58, 398–405. http://dx.doi.org/10.1016/j.optmat.2016.06.012.
Brunton, A.N., Fraser, G.W., Lees, J.E., Turcu, I.C.E., 1997. Metrology and modeling of microchannel plate x-ray optics. Appl. Opt. 36 (22), 5461–5470. http://dx.doi.org/10.1364/AO.36.005461.
Bukreeva, I., Popov, A., Pelliccia, D., Cedola, A., Dabagov, S.B., Lagomarsino, S., 2006. Wave-field formation in a hollow x-ray waveguide. Phys. Rev. Lett. 97, 184801. http://dx.doi.org/10.1103/PhysRevLett.97.184801.
Bulanov, S.V., Kirsanov, V., Sakharov, A.S., 1990. The ultrarelativistic theory of laser accelerator with wakewave. Sov. J. Plasma Phys. 16, 543.
Cappuccio, G., Dabagov, S., Pifferi, A., Gramaccioni, C., 2001. Divergence behaviour due to surface channeling in capillary optics. Appl. Phys. Lett. 78 (19), 2822–2824.
Carrigan, R.A., 1975. Single crystals and short-lived particles. Phys. Rev. Lett. 35, 206–209. http://dx.doi.org/10.1103/PhysRevLett.35.206.
Carrigan Jr.R.A., Ellison, J.A. (Eds.), 1987. Relativistic Channeling. Plenum Press, New York.
Chapman, H.N., Nugent, K.A., Wilkins, S.W., Davis, T.J., 1990. Focusing and collimation of x rays using microchannel plates: an experimental investigation. J. X-Ray Sci. Technol. 2 (2), 117–126. http://dx.doi.org/10.1016/0895-3996(90)90005-7.
Chapman, H.N., Nugent, K.A., Wilkins, S.W., 1993. X-ray focusing using cylindrical-channel capillary arrays. I. Theory. Appl. Opt. 32 (31), 6316–6332. http://dx.doi.org/10.1364/AO.32.006316.
Cherepennikov, Y., Miloichikova, I., Gogolev, A., Stuchebrov, S., Hampai, D., Dabagov, S.B., Liedl, A., 2017. Application of polycapillary optics for dual energy spectroscopy based on a laboratory source. Nucl. Instrum. Methods B 402, 278–281. http://dx.doi.org/10.1016/j.nimb.2017.03.118.
Childs, P., O'Neill, A., 2003. Propagation of x-rays in carbon nanotubes. Phys. E: Low-Dimens. Syst. Nanostruct. 19 (1), 153–156. http://dx.doi.org/10.1016/S1386-9477(03)00311-4.
Dabagov, S., Okotrub, A., 2004. On coherent scattering of x-rays in carbon nanotubes. Spectrochim. Acta Part B: At. Spectrosc. 59 (10), 1575–1580. http://dx.doi.org/10.1016/j.sab.2004.03.018.
Dabagov, S.B., 2003a. Channeling of neutral particles in micro- and nanocapillaries. Phys. Uspekhi (Rev. Top. Probl.) 46 (10), 1053–1075.
Dabagov, S.B., 2003b. Wave theory of x-ray scattering in capillary structures. X-Ray Spectrom. 32 (3), 179–185. http://dx.doi.org/10.1002/xrs.593.
Dabagov, S.B., 2011. On x-ray and neutron channeling in carbon nanotubes. Nanosci. Nanotechnol. Lett. 3 (1), 24–27.
Dabagov, S.B., Kalashnikov, N.P., 2017. On stimulated resonance radiation by channeled particles. Nucl. Instrum. Methods B 402, 67–70. http://dx.doi.org/10.1016/j.nimb.2017.03.145.
Dabagov, S.B., Uberall, H., 2007. On X-raywaveguiding in nanochannels: channeling formalism. Nucl. Instrum. Methods Phys. Res. Sect. A: Accel. Spectrometers Detect. Assoc. Equip. 580 (1), 756–763. http://dx.doi.org/10.1016/j.nima.2007.05.101.
Dabagov, S.B., Uberall, H., 2008. On X-ray channeling in narrow guides. Nucl. Instrum. Methods B 266 (17), 3881–3887. http://dx.doi.org/10.1016/j.nimb.2008.03.238.
Dabagov, S.B., Zhevago, N.K., 2008. On radiation by relativistic electrons and positrons channeled in crystals. La Riv. Nuovo Cim. 31 (9), 491–529.
Dabagov, S.B., Kumakhov, M.A., Nikitina, S.V., et al., 1995a. Observation of interference effects at the focus of an x-ray lens. J. Synch. Rad. 2, 132–135.
Dabagov, S.B., Kumakhov, M.A., Nikitina, S.V., 1995b. On the interference of x-rays in multiple reflection optics. Phys. Lett. A203, 279–282.
Dabagov, S.B., Marcelli, A., Murashova, V.A., Svyatoslavsky, N.L., Fedorchuk, R.V., Yakimenko, M.N., 2000. Coherent and incoherent components of a synchrotron radiation spot produced by separate capillaries. Appl. Opt. 39 (19), 3338–3343. http://dx.doi.org/10.1364/AO.39.003338.
Dabagov, S.B., Dik, A.V., Frolov, E.N., 2015. Channeling of electrons in a crossed laser field. Phys. Rev. ST - Accel. Beams 18 (6), 064002. http://dx.doi.org/10.1103/physrevstab.18.064002.
Dabagov, S., Capitolo, E., Gogolev, A., Hampai, D., Liedl, A., Polese, C., 2016. Parametric x-ray detection in UA9 experiment, Preprint INFN-16-05/LNF, INFN LNF, 〈http://www.lnf.infn.it/sis/:http://arXiv.org/abs//pdf/getfile.php?Filename=INFN-16-05-LNF.pdf〉(17 March).
Dabagov, S.B., (Ed.), Proceedings of the Channeling conferences for the period of 2004–2016, proc. of SPIE 5974 (2005); Proc. of SPIE 6634 (2007); of the 51st Workshop of the INFN Eloisatron Project, World Scientific, (2010); Nuovo Cimento C 34 (4) (2011); Nucl. Instr. Meth. B309 (2013); Nucl. Instr. Meth. B355 (2015); Nucl. Instr. Meth. B402 (2017).
Dabagov, S.B., 1992. Redistribution of x-rays trapped in bound states by capillarysystems, Preprint IROS-1/1992, IROS, Nalchik-Moscow.
Dabagov, S.B., 2018. Advanced channelingtechnologies in plasma and laser fields, EPJ Web of Conferences 167, 01002. 〈http://dx.doi.org/10.1051/epjconf/201816701002〉.
Dabagov, S.B., Grilli, A., Okotrub, A., 2003. Features of x-ray scattering in a nanotube layer. In: A. Bianconi, A. Marcelli, N. L. Saini (Eds.), Frascati Physics Series, Vol. XXXII, INFN, Frascati, pp. 281–294.
Dabagov, S.B., Kumakhov, M.A., 1995. X-ray channeling in capillary systems. In: Hoover, R.B., Walker, A.B., (Eds.), X-Ray and Extreme Ultraviolet Optics, Vol. 2515 of Proceedings of SPIE, SPIE, pp. 124–136.
Dabagov, S.B., Marcelli, A., Kumakhov, M.A., 2000. Channeling of neutrons in polycapillaries: a new way to bend neutrons at large angles. In: M. A. Kumakhov (Ed.), Kumakhov Optics and Applications SPIE Selected Papers, Vol. 4155, pp. 86–92. 〈http://dx.doi.org/10.1117/12.387862〉.

Dabagov, S.B., Murashova, V.A., Svyatoslavsky, N.L., Fedorchuk, R.V., Yakimenko, M.N., 1998. Features of synchrotron radiation focusing by separate capillaries of definite geometry. In: Hoover, R.B., Walker, A.B.C., (Eds.), X-Ray Optics, Instruments, and Missions, vol. 3444 of Proceedings of SPIE, SPIE, pp. 486–492.

Dabagov, S.B., Strikhanov, M.N., (Eds.), Charged & Neutral Particles Channeling Phenomena, MEPhI Pub., Moscow, ISBN 978-5-7262–1864-9 (2013); ISBN-978-5-7262–2232-5 (2016).

Davies, J., 1974. Lectures on Channelling Ion Implantation and Atomic Collisions. Physics, Tata Institute of Fundamental Research.

Dedkov, G.V., 1998. Fullerene nanotubes can be used when transporting gamma-quanta, neutrons, ion beams and radiation from relativistic particles. Nucl. Instrum. Methods B 143 (4), 584–590.

Dik, A., Dabagov, S., Frolov, E., 2016. Cooling of ultra relativistic β and μ particles by laser channels. J. Phys.: CS 732, 012002. http://dx.doi.org/10.1088/1742-6596/732/1/012002.

Dik, A., Frolov, E., Dabagov, S., 2018. On a quantum particle in laser channels. J. Instrum. 13 (02), C02018. http://dx.doi.org/10.1088/1748-0221/13/02/C02018.

Dik, A.V., Dabagov, S.B., 2013. Distribution function of electrons in an ion channel. Russ. Phys. J. 55 (12), 1402–1409. http://dx.doi.org/10.1007/s11182-013-9973-z.

Dik, A.V., Ligidov, A.Z., Dabagov, S.B., 2013. Radiation by electrons channeled in a plasma-ion cavity. Nucl. Instrum. Methods B 309, 210–213. http://dx.doi.org/10.1016/j.nimb.2013.03.014.

Engström, P., Larsson, S., Rindby, A., Buttkewitz, A., Garbe, S., Gaul, G., Knöchel, A., Lechtenberg, F., 1991. A submicron synchrotron x-ray beam generated by capillary optics. Nucl. Instrum. Methods A 302 (3), 547–552. http://dx.doi.org/10.1016/0168-9002(91)90373-X.

Esarey, E., Shadwick, B.A., Catravas, P., Leemans, W.P., 2002. Synchrotron radiation from electron beams in plasma-focusing channels. Phys. Rev. E 65, 056505. http://dx.doi.org/10.1103/PhysRevE.65.056505.

Esarey, E., Schroeder, C., Leemans, P., 2009. Physics of laser-driven plasma-based electron accelerators. Rev. Mod. Phys. 81, 1229–1285. http://dx.doi.org/10.1103/RevModPhys.81.1229.

Faure, J., Glinec, Y., Pukhov, A., Kiselev, S., Gordienko, S., Lefebvre, E., Rousseau, J.-P., Burgy, F., Malka, V., 2004. A laser-plasma accelerator producing monoenergetic electron beams. Nature 431, 541–544. http://dx.doi.org/10.1038/nature02963.

Faure, J., Rechatin, C., Lundh, O., Ammoura, L., Malka, V., 2010. Injection and acceleration of quasimonoenergetic relativistic electron beams using density gradients at the edges of a plasma channel. Phys. Plasmas 17 (8), 083107.

Fedorov, M.V., Oganesyan, K.B., Prokhorov, A.M., 1988. Free electron laser based on the effect of channeling in an intense standing light wave. Appl. Phys. Lett. 53 (5), 353–354. http://dx.doi.org/10.1063/1.99912.

Frolov, E., Dik, A., Dabagov, S., 2018. Relativistic charged particle ejection from optical lattice. J. Instrum. 13 (03), C03042. http://dx.doi.org/10.1088/1748-0221/13/03/C03042.

Frolov, E.N., Dik, A.V., Dabagov, S.B., 2013. Dynamics of electrons acceleration in presence of crossed laser field. Nucl. Instrum. Methods B 309, 157–161. http://dx.doi.org/10.1016/j.nimb.2013.03.017.

Frolov, E.N., Dik, A.V., Dabagov, S.B., 2017. Space charge effect simulation at electrons channeling in laser fields. Nucl. Instrum. Methods B 402, 220–222. http://dx.doi.org/10.1016/j.nimb.2017.03.151.

Frolov, E.N., Dik, A.V., Dabagov, S.B., 2014. Radiation of a laser-channeled electron, J. Phys.: Conf. Ser. 517 (1) 012002. ⟨http://dx.doi.org/10.1088/1742-6596/517/1/012002⟩.

Gemmell, D.S., 1974. Channeling and related effects in the motion of charged particles through crystals. Rev. Mod. Phys. 46 (1), 129–227.

Hampai, D., Dabagov, S., Cappuccio, G., Longoni, A., Frizzi, T., Cibin, G., Guglielmotti, V., Sessa, V., 2008. Elemental mapping and microimaging by x-ray capillary optics. Opt. Lett. 33 (23), 2743–2745.

Hampai, D., Dabagov, S.B., Cappuccio, G., Cibin, G., Sessa, V., 2009. X-ray micro-imaging by capillary optics. Spectrochim. Acta Part B: At. Spectrosc. 64 (11), 1180–1184. http://dx.doi.org/10.1016/j.sab.2009.08.006.

Hampai, D., Dabagov, S.B., Ventura, G.D., Bellatreccia, F., Magi, M., Bonfigli, F., Montereali, R.M., 2011. High-resolution x-ray imaging by polycapillary optics and lithium fluoride detectors combination. Europhys. Lett. 96 (6), 60010. http://dx.doi.org/10.1209/0295-5075/96/60010.

Hampai, D., Marchitto, L., Dabagov, S.B., Allocca, L., Alfuso, S., Innocenti, L., 2013a. Desktop X-ray tomography for low contrast samples. Nucl. Instrum. Methods B 309, 264–267. http://dx.doi.org/10.1016/j.nimb.2013.03.051.

Hampai, D., Bonfigli, F., Dabagov, S.B., Montereali, R.M., Ventura, G.D., Bellatreccia, F., Magi, M., 2013b. LiF detectors-polycapillary lens for advanced X-ray imaging. Nucl. Instrum. Methods A 720, 113–115. http://dx.doi.org/10.1016/j.nima.2012.12.022.

Hampai, D., Liedl, A., Polese, C., Cappuccio, G., Dabagov, S.B., 2015. RXR: a new X-ray facility at XLab Frascati. X-Ray Spectrom. 44 (4), 243–247. http://dx.doi.org/10.1002/xrs.2614.

Hampai, D., Liedl, A., Cappuccio, G., Capitolo, E., Iannarelli, M., Massussi, M., Tucci, S., Sardella, R., Sciancalepore, A., Polese, C., Dabagov, S.B., 2017. 2D-3D uXRF elemental mapping of archeological samples. Nucl. Instrum. Methods B 402, 274–277. http://dx.doi.org/10.1016/j.nimb.2017.04.020.

Hampai, D., Cherepennikov, Y.M., Liedl, A., Cappuccio, G., Capitolo, E., Iannarelli, M., Azzutti, C., Gladkikh, Y.P., Marcelli, A., Dabagov, S.B., 2018. Polycapillary based μXRF station for 3D colour tomography. J. Instrum. 13 (04), C04024. http://dx.doi.org/10.1088/1748-0221/13/04/C04024.

Ioffe, A., Dabagov, S., Kumakhov, M., 1995. Effective neutron bending at large angles. Neutron News 6 (3), 20–21. http://dx.doi.org/10.1080/10448639508217696.

Kaaret, P., Geissbuhler, P., Chen, A., Glavinas, E., 1992. X-ray focusing using microchannel plates. Appl. Opt. 31 (34), 7339–7343. http://dx.doi.org/10.1364/AO.31.007339.

Kalashnikov, N.P., 1988. Coherent Interactions of Charged Particles in Single Crystals. Scattering and Radiative Processes in Single Crystals. Harwood Acad. Pub, London - New York.

Kapitza, P., Dirac, P., 1933. The reflection of electrons from standing light waves. Math. Proc. Camb. 29, 297–300. http://dx.doi.org/10.1017/S0305004100011105.

Kaplan, A.E., Pokrovsky, A.L., 2005. Fully relativistic theory of the ponderomotive force in an ultraintense standing wave. Phys. Rev. Lett. 95, 053601. http://dx.doi.org/10.1103/PhysRevLett.95.053601.

Karabarbounis, A., Sarros, S., Trikalinos, C., 2013. Channeling and energy losses of 10 MeV protons in straight chiral carbon nanotube bundles. Nucl. Instrum. Methods B 316, 160–170. http://dx.doi.org/10.1016/j.nimb.2013.09.009.

Klimov, V., Letokhov, V., 1996. Hard X-radiation emitted by a charged particle moving in a carbon nanotube. Phys. Lett. A 222 (6), 424–428. http://dx.doi.org/10.1016/S0375-9601(96)00674-3.

Korotchenko, K., Eikhorn, Y., Dabagov, S., 2017. Fine features of parametric x-ray radiation by relativistic electrons and ions. Phys. Lett. B 774, 470–475. http://dx.doi.org/10.1016/j.physletb.2017.09.088.

Kostyukov, I., Kiselev, S., Pukhov, A., 2003. X-ray generation in an ion channel. Phys. Plasmas 10, 4818.

Kostyukov, I., Pukhov, A., Kiselyov, S., 2006. Strongly nonlinear mode interaction of laser impulse with plasma: generation of an electromagnetic radiation and ultra-relativistic electrons. Appl. Phys. 6, 35–49 (in Russian).

Kukhlevsky, S.V., Flora, F., Marinai, A., Nyitray, G., Ritucci, A., Palladino, L., Reale, A., Tomassetti, G., 2000. Diffraction of x-ray beams in capillary waveguides. Nucl. Instrum. Methods B 168 (2), 276–282. http://dx.doi.org/10.1016/S0168-583X(99)00874-5.

Kumakhov, M., 1976. On the theory of electromagnetic radiation of charged particles in a crystal. Phys. Lett. A 57 (1), 17–18. http://dx.doi.org/10.1016/0375-9601(76)90438-2.

Kumakhov, M.A., Komarov, F.F., 1989. Radiation from Charged Particles in Solids. AIP, New York.

Kumakhov, M.A., Komarov, F.F., 1990. Multiple reflection from surface x-ray optics. Phys. Rep. 191 (5), 289–350. http://dx.doi.org/10.1016/0370-1573(90)90135-O.

Kumakhov, M.A., Sharov, V.A., 1992. A neutron lens. Nature 357, 390. http://dx.doi.org/10.1038/357390a0.

Kumakhov, M.A., Shirmer, G., 1979. Atomic Collisions in Crystals. G. & B. Sci. Pub. Ltd., London.

Liedl, A., Polese, C., Hampai, D., Ventura, G.D., Dabagov, S.B., Marcelli, A., Bellatreccia, F., Cavallo, A., 2015. X-ray micro-computed tomography and micro x-ray fluorescence mapping of synthetic emerald by using a laboratory polycapillary optics x-ray tube layout. X-Ray Spectrom. 44 (4), 201–203. http://dx.doi.org/10.1002/xrs.2600.

Lindhard, J., Influence of crystal lattice on motion of energetic charged particles, Kgl. Dan. Vid. Selsk. Mat.-Fys. Medd. 34 (14).

Liu, C., Golovchenko, J.A., 1997. Surface trapped xrays: whispering-gallery modes at $\lambda = 0.7$Å. Phys. Rev. Lett. 79, 788–791. http://dx.doi.org/10.1103/PhysRevLett.79.788.

Lutz, H., Sizmann, R., 1963. Super ranges of fast ions in copper single crystals. Phys. Lett. 5 (2), 113–114.

MacDonald, C.A., 2010. Focusing polycapillaryoptics and their applications. X-Ray Optics Instrum. 867049, 1–17. http://dx.doi.org/10.1155/2010/867049.

Maksyuta, N.V., Vysotskii, V.I., Dabagov, S.B., 2017. Protonium atoms generation at antiprotons channeling in a LiH crystal. Nucl. Instrum. Methods B 402, 232–235. http://dx.doi.org/10.1016/j.nimb.2017.03.075.

Mangles, S.P.D., Walton, B.R., Tzoufras, M., Najmudin, Z., Clarke, R.J., Dangor, A.E., Evans, R.G., Fritzler, S., Gopal, A., Hernandez-Gomez, C., Mori, W.B., Rozmus, W., Tatarakis, M., Thomas, A.G.R., Tsung, F.S., Wei, M.S., Krushelnick, K., 2005. Electron acceleration in cavitated channels formed by a petawatt laser in low-density plasma. Phys. Rev. Lett. 94 (24), 245001–245004.

Marchitto, L., Hampai, D., Dabagov, S.B., Allocca, L., Polese, C., Liedl, A., 2015. GDI spray structure analysis by polycapillary X-ray μ-tomography, Intern. J. Multiph. Flow 70, 15–21. http://dx.doi.org/10.1016/j.ijmultiphaseflow.2014.11.015.

Marchitto, L., Dabagov, S.B., Allocca, L., Hampai, D., Liedl, A., Alfuso, S., 2013. X-ray tomography of high pressure fuel spray by polycapillary optics. In: Khounsary, A., Goto, S., Morawe, C., (Eds.), Advances in X-Ray/EUV Optics and Components VIII, vol. 8848 of Proceedings of SPIE, SPIE, p. 884808.

Mazuritskiy, M., Dabagov, S., Lerer, A., Dziedzic-Kocurek, K., Sokolov, A., Coreno, M., Turchini, S., D'Elia, A., Sacchi, M., Marcelli, A., 2017. Transmission diffractive patterns of large microchannel plates at soft x-ray energies. Nucl. Instrum. Methods B 402, 282–286. http://dx.doi.org/10.1016/j.nimb.2017.02.075.

Mazuritskiy, M.I., Dabagov, S.B., Dziedzic-Kocurek, K., Marcelli, A., 2013. X-ray spectroscopy of fluorescence radiation channeling in μ-capillary holed glass plates. Nucl. Instrum. Methods B 309, 240–243. http://dx.doi.org/10.1016/j.nimb.2013.02.017.

Mazuritskiy, M.I., Dabagov, S.B., Marcelli, A., Lerer, A., Novakovich, A., Dziedzic-Kocurek, K., 2014. Wave propagation of induced radiation in microcapillary holes of a glass microchannel plate. J. Opt. Soc. Am. B 31 (9), 2182–2187. http://dx.doi.org/10.1364/JOSAB.31.002182.

Mazuritskiy, M.I., Dabagov, S.B., Marcelli, A., Dziedzic-Kocurek, K., Lerer, A.M., 2015. X-ray radiation channeling in micro-channel plates: spectroscopy with a synchrotron radiation beam. Nucl. Instrum. Methods B 355, 293–296. http://dx.doi.org/10.1016/j.nimb.2015.02.033.

Mazuritskiy, M.I., Dabagov, S.B., Marcelli, A., Lerer, A.M., Dziedzic-Kocurek, K., 2016. Excitation and propagation of X-ray fluorescence through thin devices with hollowed ordered structures: comparison of experimental and theoretical spectra. J. Synchrotron Radiat. 23 (1), 274–280. http://dx.doi.org/10.1107/S1600577515020238.

Mazzolari, A., Bagli, E., Bandiera, L., Guidi, V., Backe, H., Lauth, W., Tikhomirov, V., Berra, A., Lietti, D., Prest, M., Vallazza, E., De Salvador, D., 2014. Steering of a Sub-GeV electron beam through planar channeling enhanced by rechanneling. Phys. Rev. Lett. 112, 135503. http://dx.doi.org/10.1103/PhysRevLett.112.135503.

Mourou, G., Barty, C., Perry, M., 1998. Ultrahigh-intensity lasers: physics of the extreme on a tabletop. Phys. Today 51 (1), 22–28.

Ohtsuki, Y.-H., 1983. Charged Beam Interaction with Solids. Taylor & Francis Ltd, London-New York.

Okotrub, A.V., Dabagov, S.B., Kudashov, A.G., Gusel'nikov, A.V., Kinloch, I., Windle, A.H., Chuvilin, A.L., Bulusheva, L.G., 2005. Orientational effect of the texture of a carbon-nanotube film on ckα a radiation intensity. J. Exp. Theor. Phys. Lett. 81 (1), 34–38. http://dx.doi.org/10.1134/1.1881732.

Panknin, S., Hartmann, A.K., Salditt, T., 2008. X-ray propagation in tapered waveguides: simulation and optimization. Opt. Commun. 281 (10), 2779–2783. http://dx.doi.org/10.1016/j.optcom.2008.01.013.

Piercy, G.R., Brown, F., Davies, J.A., McCorgo, M., 1963. Experimental evidence for the increase of heavy ions ranges by channeling in crystalline structure. Phys. Rev. Lett. 10 (9), 399–400.

Pogossian, S.P., Gall, H.L., 1995. Neutron andx-ray propagation laws in thin film waveguides. Opt. Commun. 114 (3), 235–241. http://dx.doi.org/10.1016/0030-4018(94)00567-E.

Pokrovsky, A.L., Kaplan, A.E., 2005. Relativistic reversal of the ponderomotive force in a standing laser wave. Phys. Rev. A 72 (4), 043401. http://dx.doi.org/10.1103/PhysRevA.72.043401.

Polese, C., Dabagov, S.B., Esposito, A., Hampai, D., Gorghinian, A., Liedl, A., Ferretti, M., 2014. Experimental study for the feasibility of using hard x-rays for micro-xrf analysis of multilayered metals. AIP Adv. 4, 077128. http://dx.doi.org/10.1063/1.4891523.

Robinson, M., Oen, O., 1963. Computer studies of the slowing down of energetic atoms in crystals. Phys. Rev. 132 (6), 2385–2398.

Rullhusen, P., Artru, X., Dhez, P., 1998. Novel Radiation Sources Using Relativistic Electrons: From Infrared to X-Rays (Series in Mathematical Biology and Medicine). World Scientific, Singapore.

Saenz, A., Uberall, H. (Eds.), 1985. Coherent Radiation Sources. Springer.

Salditt, T., Hoffmann, S., Vassholz, M., Haber, J., Osterhoff, M., Hilhorst, J., 2015. X-ray optics on a chip: guiding X rays in curved channels. Phys. Rev. Lett. 115, 203902. http://dx.doi.org/10.1103/PhysRevLett.115.203902.

Scandale, W., Arduini, G., Assmann, R., Cerutti, F., Gilardoni, S., Christiansen, J., Laface, E., Losito, R., Masi, A., Metral, E., Mirarchi, D., Montesano, S., Previtali, V., Redaelli, S., Valentino, G., Schoofs, P., Smirnov, G., Tlustos, L., Bagli, E., Baricordi, S., Dalpiaz, P., Guidi, V., Mazzolari, A., Vincenzi, D., Buonomo, B., Dabagov, S., Murtas, F., Carnera, A., Mea, G.D., Salvador, D.D., Lombardi, A., Lytovchenko, O., Tonezzer, M., Cavoto, G., Ludovici, L., Santacesaria, R., Valente, P., Galluccio, F., Afonin, A., Bulgakov, M., Chesnokov, Y., Maisheev, V., Yazynin, I., Kovalenko, A., Taratin, A., Gavrikov, Y., Ivanov, Y., Lapina, L., Skorobogatov, V., Ferguson, W., Fulcher, J., Hall, G., Pesaresi, M., Raymond, M., Rose, A., Ryan, M., Zorba, O., Robert-Demolaize, G., Markiewicz, T., Oriunno, M., Wienands, U., Efremov, Y., Uglov, S., Gogolev, A., 2011a. Observation of parametric x-rays produced by 400 GeV/c protons in bent crystals. Phys. Lett. B 701 (2), 180–185. http://dx.doi.org/10.1016/j.physletb.2011.05.060.

Scandale, W., Arduini, G., Assmann, R., Bracco, C., Cerutti, F., Christiansen, J., Gilardoni, S., Laface, E., Losito, R., Masi, A., Metral, E., Mirarchi, D., Montesano, S., Previtali, V., Redaelli, S., Valentino, G., Schoofs, P., Smirnov, G., Tlustos, L., Bagli, E., Baricordi, S., Dalpiaz, P., Guidi, V., Mazzolari, A., Vincenzi, D., Dabagov, S., Murtas, F., Carnera, A., Mea, G.D., Salvador, D.D., Lombardi, A., Lytovchenko, O., Tonezzer, M., Cavoto, G., Ludovici, L., Santacesaria, R., Valente, P., Galluccio, F., Afonin, A., Bulgakov, M., Chesnokov, Y., Maisheev, V., Yazynin, I., Kovalenko, A., Taratin, A., Uzhinskiy, V., Gavrikov, Y., Ivanov, Y., Lapina, L., Skorobogatov, V., Ferguson, W., Fulcher, J., Hall, G., Pesaresi, M., Raymond, M., Rose, A., Ryan, M., Zorba, O., Robert-Demolaize, G., Markiewicz, T., Oriunno, M., Wienands, U., 2011b. Comparative results on collimation of the sps beam of protons and pb ions with bent crystals. Phys. Lett. B 703 (5), 547–551. http://dx.doi.org/10.1016/j.physletb.2011.08.023.

Scandale, W., Arduini, G., Butcher, M., Cerutti, F., Gilardoni, S., Lari, L., Lechner, A., Losito, R., Masi, A., Mereghetti, A., Metral, E., Mirarchi, D., Montesano, S., Redaelli, S., Schoofs, P., Smirnov, G., Bagli, E., Bandiera, L., Baricordi, S., Dalpiaz, P., Guidi, V., Mazzolari, A., Vincenzi, D., Claps, G., Dabagov, S., Hampai, D., Murtas, F., Cavoto, G., Garattini, M., Iacoangeli, F., Ludovici, L., Santacesaria, R., Valente, P., Galluccio, F., Afonin, A., Bulgakov, M., Chesnokov, Y., Maisheev, V., Yazynin, I., Kovalenko, A., Taratin, A., Uzhinskiy, V., Gavrikov, Y., Ivanov, Y., Lapina, L., Ferguson, W., Fulcher, J., Hall, G., Pesaresi, M., Raymond, M., Previtali, V., 2013. Optimization of the crystal assisted collimation of the sps beam. Phys. Lett. B 726 (1), 182–186. http://dx.doi.org/10.1016/j.physletb.2013.08.028.

Scandale, W., Arduini, G., Butcher, M., Cerutti, F., Gilardoni, S., Lari, L., Lechner, A., Losito, R., Masi, A., Mereghetti, A., Metral, E., Mirarchi, D., Montesano, S., Redaelli, S., Schoofs, P., Smirnov, G., Bagli, E., Bandiera, L., Baricordi, S., Dalpiaz, P., Guidi, V., Mazzolari, A., Vincenzi, D., Claps, G., Dabagov, S., Hampai, D., Murtas, F., Cavoto, G., Garattini, M., Iacoangeli, F., Ludovici, L., Santacesaria, R., Valente, P., Galluccio, F., Afonin, A., Chesnokov, Y., Maisheev, V., Sandomirskiy, Y., Yanovich, A., Yazynin, I., Kovalenko, A., Taratin, A., Gavrikov, Y., Ivanov, Y., Lapina, L., Ferguson, W., Fulcher, J., Hall, G., Pesaresi, M., Raymond, M., Previtali, V., 2014a. Deflection of high energy protons by multiple volume reflections in a modified multi-strip silicon deflector. Nucl. Instrum. Methods B 338, 108–111. http://dx.doi.org/10.1016/j.nimb.2014.08.013.

Scandale, W., Arduini, G., Butcher, M., Cerutti, F., Gilardoni, S., Lechner, A., Losito, R., Masi, A., Metral, E., Mirarchi, D., Montesano, S., Redaelli, S., Smirnov, G., Bagli, E., Bandiera, L., Baricordi, S., Dalpiaz, P., Germogli, G., Guidi, V., Mazzolari, A., Vincenzi, D., Claps, G., Dabagov, S., Hampai, D., Murtas, F., Cavoto, G., Garattini, M., Iacoangeli, F., Ludovici, L., Santacesaria, R., Valente, P., Galluccio, F., Afonin, A., Chesnokov, Y., Chirkov, P., Maisheev, V., Sandomirskiy, Y., Yazynin, I., Kovalenko, A., Taratin, A., Gavrikov, Y., Ivanov, Y., Lapina, L., Ferguson, W., Fulcher, J., Hall, G., Pesaresi, M., Raymond, M., 2014b. Mirroring of 400 gev/c protons by an ultra-thin straight crystal. Phys. Lett. B 734, 1–6. http://dx.doi.org/10.1016/j.physletb.2014.04.062.

Scandale, W., Arduini, G., Butcher, M., Cerutti, F., Gilardoni, S., Lechner, A., Losito, R., Masi, A., Metral, E., Mirarchi, D., Montesano, S., Redaelli, S., Smirnov, G., Bandiera, L., Baricordi, S., Dalpiaz, P., Guidi, V., Mazzolari, A., Vincenzi, D., Claps, G., Dabagov, S., Hampai, D., Murtas, F., Cavoto, G., Garattini, M., Iacoangeli, F., Ludovici, L., Santacesaria, R., Valente, P., Galluccio, F., Afonin, A., Chesnokov, Y., Chirkov, P., Maisheev, V., Sandomirskiy, Y., Yazynin, I., Kovalenko, A., Taratin, A., Gavrikov, Y., Ivanov, Y., Lapina, L., Ferguson, W., Fulcher, J., Hall, G., Pesaresi, M., Raymond, M., 2014c. Observation of focusing of 400 gev/c proton beam with the help of bent crystals. Phys. Lett. B 733, 366–372. http://dx.doi.org/10.1016/j.physletb.2014.05.010.

Scandale, W., Arduini, G., Butcher, M., Cerutti, F., Garattini, M., Gilardoni, S., Lechner, A., Losito, R., Masi, A., Mereghetti, A., Metral, E., Mirarchi, D., Montesano, S., Redaelli, S., Rossi, R., Schoofs, P., Smirnov, G., Bagli, E., Bandiera, L., Baricordi, S., Dalpiaz, P., Germogli, G., Guidi, V., Mazzolari, A., Vincenzi, D., Claps, G., Dabagov, S., Hampai, D., Murtas, F., Cavoto, G., Iacoangeli, F., Ludovici, L., Santacesaria, R., Valente, P., Galluccio, F., Afonin, A., Chesnokov, Y., Durum, A., Maisheev, V., Sandomirskiy, Y., Yanovich, A., Kovalenko, A., Taratin, A., Gavrikov, Y., Ivanov, Y., Lapina, L., Fulcher, J., Hall, G., Pesaresi, M., Raymond, M., 2015. Observation of strong leakage reduction in crystal assisted collimation of the SPS beam. Phys. Lett. B 748, 451–454. http://dx.doi.org/10.1016/j.physletb.2015.07.040.

Scandale, W., Arduini, G., Butcher, M., Cerutti, F., Garattini, M., Gilardoni, S., Lechner, A., Losito, R., Masi, A., Mirarchi, D., Montesano, S., Redaelli, S., Rossi, R., Schoofs, P., Smirnov, G., Valentino, G., Breton, D., Burmistrov, L., Chaumat, V., Dubos, S., Maalmi, J., Puill, V., Stocchi, A., Bagli, E., Bandiera, L., Germogli, G., Guidi, V., Mazzolari, A., Dabagov, S., Murtas, F., Addesa, F., Cavoto, G., Iacoangeli, F., Ludovici, L., Santacesaria, R., Valente, P., Galluccio, F., Afonin, A., Chesnokov, Y., Durum, A., Maisheev, V., Sandomirskiy, Y., Yanovich, A., Kovalenko, A., Taratin, A., Denisov, A., Gavrikov, Y., Ivanov, Y., Lapina, L., Malyarenko, L., Skorobogatov, V., James, T., Hall, G., Pesaresi, M., Raymond, M., 2016. Observation of channeling for 6500 GeV/c protons in the crystal assisted collimation setup for LHC. Phys. Lett. B 758, 129–133. http://dx.doi.org/10.1016/j.physletb.2016.05.004.

Scandale, W., Arduini, G., Cerutti, F., Garattini, M., Gilardoni, S., Masi, A., Mirarchi, D., Montesano, S., Petrucci, S., Redaelli, S., Rossi, R., Breton, D., Burmistrov, L., Dubos, S., Maalmi, J., Natochii, A., Puill, V., Stocchi, A., Sukhonos, D., Bagli, E., Bandiera, L., Guidi, V., Mazzolari, A., Romagnoni, M., Murtas, F., Addesa, F., Cavoto, G., Iacoangeli, F., Galluccio, F., Afonin, A., Bulgakov, M., Chesnokov, Y., Durum, A., Maisheev, V., Sandomirskiy, Y., Yanovich, A., Kolomiets, A., Kovalenko, A., Taratin, A., Smirnov, G., Denisov, A., Gavrikov, Y., Ivanov, Y., Lapina, L., Malyarenko, L., Skorobogatov, V., Auzinger, G., James, T., Hall, G., Pesaresi, M., Raymond, M., 2018. Focusing of a particle beam by a crystal device with a short focal length. Nucl. Instrum. Methods B 414, 104–106. http://dx.doi.org/10.1016/j.nimb.2017.10.036.

Shintake, T., 1992. Proposal of a nanometer beamsize monitor for e + e− linear colliders. Nucl. Instrum. Methods A 311 (3), 453–464. http://dx.doi.org/10.1016/0168-9002(92)90641-G.

Spiller, E., Segmuller, A., 1974. Propagation of x rays in waveguides. Appl. Phys. Lett. 24 (2), 60–61.

Tajima, T., Dawson, J.M., 1979. Laser electron accelerator. Phys. Rev. Lett. 43, 267–270.

Thiel, D.J., Bilderback, D.H., Lewis, A., Stern, E.A., 1992. Submicron concentration and confinement of hard x-rays. Nucl. Instrum. Methods A 317 (3), 597–600. http://dx.doi.org/10.1016/0168-9002(92)91006-U.

Tsyganov, E., Some aspects of the mechanism of a charged particle penetration through a monocrystal, Fermilab TM-682, Batavia.

Vinogradov, A.V., Kovalev, V.F., Kozhevnikov, I.V., Pustovalov, V.V., 1985. Diffraction theory for grazing modes in concave mirrors and resonators at x-ray wavelengths. Sov. Phys. Tech. Phys. 30, 335–339.

Wiedemann, H., (Ed.), 2005. Advanced Radiation Sources and Applications: Proceedings of the NATO Advanced Research Workshop, held in Nor-Hamberd, Yerevan, Armenia, August 29 - September 2, 2004, NATO Science Series II:, Springer Netherlands.

Wienands, U., Markiewicz, T.W., Nelson, J., Noble, R.J., Turner, J.L., Uggerhøj, U.I., Wistisen, T.N., Bagli, E., Bandiera, L., Germogli, G., Guidi, V., Mazzolari, A., Holtzapple, R., Miller, M., 2015. Observation of deflection of a beam of multi-gev electrons by a thin crystal. Phys. Rev. Lett. 114, 074801. http://dx.doi.org/10.1103/PhysRevLett.114.074801.

Wienands, U., Gessner, S., Hogan, M., Markiewicz, T., Smith, T., Sheppard, J., Uggerhøj, U., Hansen, J., Wistisen, T., Bagli, E., Bandiera, L., Germogli, G., Mazzolari, A., Guidi, V., Sytov, A., Holtzapple, R., McArdle, K., Tucker, S., Benson, B., 2017. Channeling and radiation experiments at SLAC. Nucl. Instrum. Methods B 402, 11–15. http://dx.doi.org/10.1016/j.nimb.2017.03.097.

Zhevago, N., Glebov, V., 2003. Computer simulationsof fast particle propagation through straight and bent nanotubes. Phys. Lett. A 310 (4), 301–310. http://dx.doi.org/10.1016/S0375-9601(03)00241-X.

Zhevago, N.K., Glebov, V.I., 1998. Channeling of fast charged and neutral particles in nanotubes. Phys. Lett. 250 (4–6), 360–368.

Zwanenburg, M., Bongaerts, J., Peters, J., Riese, D., van der Veen, J., 2000. Focusing of coherent x-rays in a tapered planar waveguide. Phys. B: Condens. Matter 283 (1), 285–288. http://dx.doi.org/10.1016/S0921-4526(99)02003-7.

Zwanenburg, M.J., Peters, J.F., Bongaerts, J.H.H., de Vries, S.A., Abernathy, D.L., der Veen, J.F.V., 1999. Coherent propagation of x rays in a planar waveguide with a tunable air gap. Phys. Rev. Lett. 82 (8), 1696–1699.